# Electro-oxidation of organic pollutants by reactive electrochemical membranes

Clément Trellu, Brian Chaplin, Clémence Coetsier, Roseline Esmilaire, Sophie Annick Cerneaux, Christel Causserand, Marc Cretin

# Electro-oxidation of organic pollutants by reactive electrochemical membranes

Clément Trellu [a, c, *], Brian P. Chaplin [b], Clémence Coetsier [c], Roseline Esmilaire [a], Sophie Cerneaux [a], Christel Causserand [c], Marc Cretin [a]

[a] Institut Européen des Membranes, IEM - UMR 5635, ENSCM, CNRS, Univ Montpellier, Montpellier, France
[b] Department of Chemical Engineering, University of Illinois at Chicago, 810 S. Clinton Street, Chicago, IL 60607, USA
[c] Laboratoire de Génie Chimique, Université de Toulouse, CNRS, INPT, UPS, Toulouse, France

## HIGHLIGHTS

- Recent advances on reactive electrochemical membranes (REMs) are reviewed.
- Carbon nanotubes and $TiO_x$ materials have been the most widely studied materials.
- REMs have high electroactive surface area.
- Flow through REMs allow for convection enhanced mass transport of pollutants.
- Scientific challenges and perspectives on the development of REMs are highlighted.

## ARTICLE INFO

## ABSTRACT

Electro oxidation processes are promising options for the removal of organic pollutants from water. The major appeal of these technologies is the possibility to avoid the addition of chemical reagents. However, a major limitation is associated with slow mass transfer that reduces the efficiency and hinders the potential for large scale application of these technologies. Therefore, improving the reactor configuration is currently one of the most important areas for research and development. The recent development of a reactive electrochemical membrane (REM) as a flow through electrode has proven to be a breakthrough innovation, leading to both high electrochemically active surface area and convection enhanced mass transport of pollutants. This review summarizes the current state of the art on REMs for the electro oxidation of organic compounds by anodic oxidation. Specific focuses on the electroactive surface area, mass transport, reactivity, fouling and stability of REMs are included. Recent advances in the development of sub stoichiometric titanium oxide REMs as anodes have been made. These electrodes possess high electrical conductivity, reactivity (generation of $^{\bullet}OH$), chemical/electrochemical stability, and suitable pore structure that allows for efficient mass transport. Further development of REMs strongly relies on the development of materials with suitable physico chemical characteristics that produce electrodes with efficient mass transport properties, high electroactive surface area, high reac tivity and long term stability.

## 1. Introduction

The management of both quantity and quality of water re sources is a major environmental, health and societal concern for both developed and developing countries. For example, the Euro pean Union has raised concerns on the increasing concentrations of organic micropollutants in water bodies and imposed regulations on the discharge of organic pollutants. Most recently, the Priority Substances Directive 2013/39/EU amended the Water Framework Directive (2006/60/EC) and Directive 2008/105/EC on Environ mental Quality Standards. As another example, the United States Environmental Protection Agency placed several trace contami nants on a “Contaminant Candidate List”, for which information on

occurrence and health effects must be monitored. Efficient water management is also becoming an important economic concern for industrial activities, and as a result water reuse is being implemented by several industrial sectors. To meet the challenges of water quality and quantity, the development of compact, robust and cost effective technologies for the treatment of domestic and industrial effluents containing recalcitrant organic compounds is needed (Joss et al., 2008).

Biological processes are widely used in conventional waste water treatment systems because of their high cost effectiveness for the removal of biodegradable organic matter, nitrogen and phosphorus. However, an additional barrier using advanced water treatment technologies is required for removing non biodegradable organic pollutants from water. Ozone or UV based oxidation processes and activated carbon are the most commonly used methods for upgrading wastewater treatment plants (Joss et al., 2008). However, some organic compounds are still recalcitrant to oxidation by ozone or UV based processes and incomplete mineralization of molecules can lead to the formation of even more toxic by products. Besides, activated carbon is only a separation process, which requires subsequent waste disposal. Membrane processes have also been developed in order to create a physical barrier for the separation of suspended particles (microfiltration); bacteria, viruses, and some dissolved species (ultrafiltration and nanofiltration); or almost all dissolved species (reverse osmosis). Microfiltration and ultrafiltration processes are not able to reach sufficient removal rates of dissolved organic pollutants, and nanofiltration and reverse osmosis greatly increase operating costs, due to the high transmembrane pressures required, fouling issues, and management of the membrane concentrate (Luo et al., 2014).

The development of electrochemical processes is currently a major topic of interest in the scientific community because they are showing promise as a next generation technologies for the removal of organic compounds from water (Chaplin, 2014; Sirés et al., 2014; Martínez Huitle et al., 2015; Radjenovic and Sedlak, 2015). They have several technical benefits such as the absence of storage and handling of chemicals, an easily automated operation, as well as a compact and modular reactor design making them attractive for decentralized water and wastewater treatment systems. Anodic oxidation (AO), which is categorized as an electrochemical advanced oxidation process (EAOP), has been shown to be highly effective for the treatment of aqueous organic waste streams. The AO process is based on the removal of contaminants by a combination of direct electron transfer from the contaminant (R) to the anode (Eq. (1)) and the production of large quantities of hydroxyl radicals ($^{\bullet}OH$) from water discharge at the surface of an anode material (M) with high $O_2$ overpotential (Eq. (2)), such as boron doped diamond (Panizza and Cerisola, 2009). The $^{\bullet}OH$ is both a very strong oxidant (the thermodynamic potential of $^{\bullet}OH$ formation is $E^{\circ}$ 2.38 V *vs.* standard hydrogen electrode (SHE)) and highly reactive species allowing the degradation of a wide range of bio refractory organic compounds (Eq. (3)) (Buxton et al., 1988; Kapałka et al., 2009). Many examples of total mineralization of various organic pollutants and complex effluents have been reported in the scientific literature and comparative studies often indicated that higher mineralization of organic compounds was achieved with AO compared to other advanced oxidation processes (Comninellis and Nerini, 1995; Rodrigo et al., 2001; Canizares et al., 2003; Brillas et al., 2005, 2007; Ozcan et al., 2008; Panizza and Cerisola, 2009; Fernandes et al., 2012; Oturan et al., 2012; Chaplin, 2014; Brillas and Martínez Huitle, 2015; Trellu et al., 2016a, 2016b).

$$R \rightarrow (R)^{+} + e^{-} \quad (1)$$

$$M + H_2O \rightarrow M(^{\bullet}OH) + H^{+} + e^{-} \quad (2)$$

$$R + M(^{\bullet}OH) \rightarrow \text{degradation byproducts} \quad (3)$$

However, several scientific challenges still need to be overcome in order to promote the application of AO for water treatment. The $^{\bullet}OH$ are produced at an anode surface, and due to their short lifetime they are only present in a thin layer (<1 μm) close to the anode surface (Kapałka et al., 2008, 2009; Donaghue and Chaplin, 2013). Therefore, reactions occur at or near the electrode surface, and at currents at or above the limiting current, electrolysis is limited by mass transport of pollutants from the bulk to the electrode surface. In addition, side reactions such as the oxygen evolution reaction (OER) strongly decrease the current efficiency for target compound oxidation (Panizza et al., 2001; Panizza and Cerisola, 2009; Chaplin, 2014). Currently, most of the electrodes used in AO are conventional plate anodes implemented in parallel plate reactors, for which mass transport is strongly limited by diffusion through a thick (~10–100 μm) stagnant boundary layer (Liu and Vecitis, 2012; Zaky and Chaplin, 2013). The possibility to reach high current efficiency depends mainly on the implementation of a preconcentration step of organic pollutants by adsorption or filtration processes (Ganiyu et al., 2015). It has been shown that the most promising way to avoid diffusion/mass transfer limitations and to increase the electroactive surface area is using porous electrodes in flow through configurations (Vecitis et al., 2011; Liu and Vecitis, 2012; Zaky and Chaplin, 2013; Guo et al., 2016b). Recent results obtained during the last five years demonstrated that reactive electrochemical membranes (REMs) are a breakthrough technology for electro oxidation of organic pollutants during water treatment. Thus, REMs are becoming a major area of interest in the field of both material science and electrochemical engineering.

Although several review articles thoroughly detailed electro oxidation processes (Brillas et al., 2009; Panizza and Cerisola, 2009; Chaplin, 2014; Sirés et al., 2014; Vasudevan and Oturan, 2014; Brillas and Martínez Huitle, 2015; Martínez Huitle et al., 2015; Radjenovic and Sedlak, 2015), a summary of recent advancements related to REMs are needed. The objective of this work is to provide a state of the art on the electro oxidation of organic compounds by REMs as well as to highlight the future perspectives of this technology. The emphasis given to electro oxidation mechanisms complements the review by Ronen et al. (2016) on electro conductive and electro responsive membranes. Thus, the main focuses are to review literature related to: (i) the synthesis and characterization of REMs, (ii) the electroactive surface area of REMs (iii), the mass transport of organic pollutants in REM reactors, (iv) the charge transfer and oxidation mechanisms (direct electron transfer, mediated oxidation) using REM materials, and (v) the main issues affecting lifetime of REMs (fouling and corrosion). Finally, main conclusions and perspectives are drawn in order to establish the potential of REMs for the removal of organic pollutants from water.

## 2. Materials used as REMs

Enhancing the implementation of REMs for water treatment requires the improvement of membrane design, by a fine control of their porous structure and pore size, while maintaining high electrical conductivity, mechanical resistance, and efficient mass transport. Indeed, the morphological and physico chemical

properties of membrane materials directly affect their electro chemical activity. In this section, the synthesis and properties of carbon and semi conducting oxide based materials are described. The characteristics of the most utilized REMs have been highlighted in Tables 1 and 2, and their suitability for electro oxidation is dis cussed in the subsequent sections.

### 2.1. Carbon based REMs

Many studies utilized conductive carbon materials for the syn thesis of REMs, such as graphene (2D base unit), multi wall carbon nanotubes (MWCNTs) (1D structure) and graphite (3D structure). These materials are characterized by a $sp^2$ hybridization, allowing the delocalization of $\pi$ $\pi$ electrons in the structures and thus they possess a high theoretical conductivity (Iijima, 1991; Iijima and Ichihashi, 1993; Novoselov et al., 2004; Castro Neto et al., 2009). REMs prepared from graphene and MWCNTs mainly suffer from poor connectivity due to weak van der Waals interactions that limit their electron conductivity (Gao et al., 2014; Liu et al., 2014). However, these materials are effective at coupling adsorption and electro oxidation, due to their high specific surface area (Peigney et al., 2001).

Yang et al. (2009) evaluated MWCNTs packed between two pieces of activated carbon felts that formed a porous cathode anode cell, that was utilized as a seepage MWCNT electrode reactor. Vecitis et al. (2011) proposed another original design of an electrochemical filter using CNTs (Fig. 1 a), which had improved electrochemical and filtration characteristics. In this design, a CNT layer (Fig. 1 b) was deposited by vacuum filtration on a polytetra fluoroethylene (PTFE) filter support (pore diameter of 5 μm) without using a binder (Fig. 1 c and 1 d).

However, CNT based REMs can be leached into solution during the filtration process (Gao et al., 2014), which is a major issue for water treatment applications because of the cytotoxicity of CNTs (Shvedova et al., 2003). Therefore, researchers also prepared com posite CNT materials using polymers binders such as poly vinylidene fluoride (PVDF) (Gao et al., 2014) and polyaniline (PANI) (Wang et al., 1987; Duan et al., 2016), which prevented the CNT release and increased the REM stability and electron conductivity. A similar strategy was utilized with carbon nanofibers (CNFs), which were dispersed in a polyethersulfone (PES) matrix and deposited on an ultrafiltration polymer support (Li et al., 2017).

In summary, CNTs appear to be the most promising carbon materials to fabricate REMs due to their small pores size, high porosity, high specific surface area, and their tunable properties by incorporation of binders (polymer, conductive polymer, and gra phene). Subsequent research should focus on nanostructuring of CNT filters, for example with lithographic technics to synthesize uniform and vertically aligned CNTs (Prasek et al., 2011).

### 2.2. Ceramic membranes

A review of the literature suggests that oxides are very prom ising materials for the fabrication of REMs. In contrast to CNT and graphene REMs, ceramic processing allows the large scale fabri cation of REMs with various shapes, fine control of the pore size and effective grain boundaries during the sintering step. Recent works were focused on developing porous and electrocatalytic mem branes based on carbon or Ti membranes modified with semi conductive materials such as $TiO_2$ or $RuO_2$. Sub stoichiometric Ti oxides ($TiO_x$ or $Ti_nO_{2n-1}$ ($4 \leq n \leq 10$)), also known as Magnéli pha ses, represent the most promising oxides for REM fabrication. These oxides, which were first synthesized and characterized in the 1950s (Andersson et al., 1957), have an oxygen evolution potential (OEP) and $^{\bullet}OH$ production rate that is comparable to BDD electrodes (Bejan et al., 2009). Common stoichiometric $TiO_2$ phases (rutile, anatase, and brookite) present an n type doping at ambient con ditions, due to intrinsic defects related to oxygen vacancies ($V_O$) and interstitial titanium atoms ($Ti_i$). In the case of Magnéli phases, the conductivity arises from a restructuring of the crystal lattice to eliminate the oxygen vacancies, which results in the formation of shear planes due to rutile $TiO_2$ and corundum $Ti_2O_3$ stacking (Padilha et al., 2016). Among the different Magnéli phases, re searchers mainly focused their attention on $Ti_4O_7$, due to its high electrical conductivity ($\approx 1000\ S\ cm^{-1}$) (Smith et al., 1998). More over, $Ti_4O_7$ is insoluble in strong acids and bases and more stable than carbon under anodic polarization (Pollock et al., 1984). How ever, the conductivity of Magnéli materials can also be affected by the porosity of the material, due to contact resistance (Hayfield, 2001; Ye et al., 2015; Guo et al., 2016a). The general route to fabricate porous monolithic $Ti_4O_7$ REMs consists of the processing and sintering of a $TiO_2$ porous material (tube, plate, rod, and pellet) followed by a second thermal treatment under a reductive atmo sphere (e.g., $H_2$) (Eq. (4)).

$$4TiO_2 + H_2 \rightarrow Ti_4O_7 + H_2O \quad (4)$$

In general, the micro structure of the produced materials de pends mainly on the choice of thermal treatment temperature and duration, as well as on the mass and density of the $TiO_2$ precursor structure (Table 1) (Hayfield, 2001; Guo et al., 2016b; You et al., 2016). For example, $Ti_4O_7$ ultrafiltration membranes were synthe sized by reduction of commercial $TiO_2$ ultrafiltration membranes at 1050 °C for 50 h under $H_2$ (Guo et al., 2016b). As another example, a UF layer composed of $Ti_4O_7$ and $Ti_6O_{11}$ was obtained by dip coating of a $TiO_2$ layer on the inner surface of a tubular $Al_2O_3$ membrane, followed by a reduction step under 30% $H_2$ in Ar at 1025 °C for 7 h (Geng and Chen, 2016). A REM was also previously fabricated from a commercially available Ebonex® electrode. These macroporous ceramic Magnéli phases were prepared from the reduction of a $TiO_2$ tube under $H_2$ to yield a bimodal porous structure (Table 1), which contains a mixture of $Ti_4O_7$, $Ti_5O_9$ and $Ti_6O_{11}$ as secondary phases (Hayfield, 2001). The control of the stoichiometry of Magnéli pha ses according to the choice of precursors and thermal treatment is an interesting challenge for material science. Other chemical reducing agents may be used instead of $H_2$ in order to prepare Magnéli materials, such as Ti (Lu et al., 2012), $NH_3$ (Tang et al., 2012), Zr (Kitada et al., 2012), and carbon (Zhu et al., 2013; Trellu et al., 2018). Recently, the carbothermal reduction of $TiO_2$ proved its efficiency in the synthesis of a macroporous REM composed mainly of conductive $Ti_5O_9$ and $Ti_4O_7$ phases (Trellu et al., 2018).

Porous $Ti_4O_7$ monoliths might overcome many of the carbon materials drawbacks, since $Ti_4O_7$ can achieve good interconnection of grains (sintering process), a high stability under anodic polari zation, and the generation of hydroxyl radicals by the oxidation of water.

## 3. Electroactive surface area of REMs

The reaction of substrates with $^{\bullet}OH$ are often in the diffusion limited range with second order rate constants commonly ranging from $10^9$ to $10^{10}\ M^{-1}\ s^{-1}$ (Buxton et al., 1988). Experimental and modeling studies have also shown that due to the high reactivity of $^{\bullet}OH$, they exist in only a narrow reaction zone adjacent to the electrode surface (<1.0 μm) (Kapałka et al., 2009; Mascia et al., 2007; Donaghue and Chaplin, 2013). As a result of these very fast kinetic processes, the use of 2D electrodes, and small reaction zone volumes, the operation of electrochemical water treatment tech nologies become mass transport limited at relatively low applied current densities (e.g., $<5\ mA\ cm^{-2}$) (Canizares et al., 2006;

**Table 1**
Recapitulative table of material characteristics of REMs used for electro-oxidation of organic pollutants.

| Anode (working electrode) | Pore size (nm) | Porosity (%) | Specific surface area ($m^2$ $g^{-1}$) | Total specific surface area ($m^2$) (directly from reference or calculated) | Geometric surface area ($m^2$) | Shape | Permeability (L $h^{-1}$ $m^{-2}$ $bar^{-1}$) | Conductivity (S.$cm^{-1}$) | Reference |
|---|---|---|---|---|---|---|---|---|---|
| Porous graphite carbon | | | | | 0.0145 | Tube | | | Korbahti and Tanyolac (2003) |
| CNT/activated carbon felt (ACF) | 60 - 100 for CNT (<2 for ACF) | | 40 - 70 for CNT | 20 - 35 for CNT | 0.0028 | MWCNT on flat ACF electrodes | | | Yang et al. (2009) |
| CNT/PTFE filter | 115 ± 47 (CNT) | 85 | 88.5 | 1.05 | 0.0007 | Flat | | 102 | Vecitis et al. (2011) |
| CNT, Sb-doped $SnO_2$-coated CNT, surface-treated CNT /PTFE filters | 110 ± 10 (CNT) 136 ± 60 (after $SnO_2$/Sb coating) | 85 | 88.5 for CNT | 1.4 for CNT | 0.0007 | Flat | | 102 (CNT) | Gao and Vecitis (2011) |
| CNT, $SnO_2$-coated CNT, Sb-doped $SnO_2$-coated CNT, Bi-doped $SnO_2$-coated /PTFE filters | 110 ± 10 (CNT) | 85 | 88.5 for CNT | 1.4 for CNT | 0.0007 | Flat | | 102, 0.01 1, 1-200, | Liu et al. (2013) |
| CNT/PTFE filter | 104 ± 39 (CNT) | 85 | 88.5 | 1.4 | 0.0007 | Flat | | 102 | Gao and Vecitis (2012b) |
| CNT, B-doped CNT, N-doped CNT PTFE filters | 104 ± 39 (CNT), 112 ± 46 (B-CNT), 99 ± 42 (N-CNT), | 85 | 88.5 for CNT | 1.4 for CNT | 0.0007 | Flat | | | Gao and Vecitis (2012a) |
| CNT/PTFE filter | 104 ± 39 (CNT) | 85 | 88.5 | 1.4 | 0.0007 | Flat | | | Liu and Vecitis (2012) |
| CNT/PTFE filter | 104 ± 39 (CNT) | 85 | 88.5 | 1.4 | 0.0007 | Flat | | 102 | Schnoor and Vecitis (2013) |
| CNT/PTFE filter | 104 ± 39 (CNT) | 85 | 88.5 | 1.4 | 0.0007 | Flat | | 102 | Gao and Vecitis (2013) |
| Graphene nanoplatelet (GNP): CNT coated GNP/PTFE filter | | Inferior to CNT filter (<85) | 420 (30%wt CNT) | ≈6.7 (30%wt CNT) | 0.0007 | Flat | 2116 (pure GNP) | Low conductivity compared to isolated GNP | Liu et al. (2014) |
| CNT/PTFE filter combined with CNT-PVDF membrane | | 86 for pure CNT and 81 for CNT/ PVDF | | 1 | 0.0007 | Flat | 510 for CNT and 180 for CNT/ PVDF filter | $9.5.10^{-7}$ - $3,7.10^{-5}$ | Gao et al. (2014) |
| CNT treated CNT /PTFE filter | 104 ± 39 (CNT) | 85 | 120.7 (CNT electro-oxidized), 88.5 (CNT) | 1.9 (CNT electro-oxidized) | 0.0007 | Flat | | | Gao et al. (2015a,b) |
| CNT/PTFE filter | 110 ± 10 (CNT) | 85 | 88.5 | 1.4 | 0.0007 | Flat | | 102 | Liu et al. (2015) |
| Carbon aerogel (CA), $SnO_2$-coated carbon aerogel, Sb-doped $SnO_2$-coated carbon aerogel | 227 (CA) | 97 (CA) | 666 (CA) | 138 | 0.0002 | Flat | | | Liu et al. (2016a,b) |
| CNT, carboxylated CNT /PTFE filters | Inner diameter of 3 5 nm | | 125 (CNT), 133 (carboxylated CNT) | | 0.0007 | Flat | | >100 (reported by the manufacturer) | Bakr and Rahaman (2016) |
| CNT, B-doped CNT /PTFE filters | Inner diameter of 3 5 nm | | 166 (CNT) 60 (B-doped CNT) | | 0.0007 | Flat | | >100 (reported by the manufacturer) | Bakr and Rahaman (2017) |
| Polyaniline (PANI) coated CNT, PVA coated CNT | PANI/CNT: 20 ± 2 PVA/CNT: 46.37 ± 2.37 | $H_2SO_4$-PANI/ CNT (25%) PVA/CNT (28%) | | | 0.0004 | Flat | 3 (PANI/CNT) 2.8 (PVA/CNT) | PANI/CNT: 89.28 ± 3.07 PVA/CNT: 8.83 ± 0.24 | Duan et al. (2016) |

| | | | | | | | | | |
|---|---|---|---|---|---|---|---|---|---|
| Sb-doped $SnO_2$-coated coal-based carbon (CM) | 420 | 44.56 | | | 0.0004 | Flat | | | Liu et al. (2017) |
| $Fe^0$ NP catalyst carboxylated-CNT/PTFE filter | 24 25 | ≈80 | | | 0.0013 | Flat | 220 | 13 17 | Yanez et al. (2017) |
| Carbon nanofibers/PES composite forward osmosis membrane | | 62.4 ± 2.4 | | | 0.0002 0.0020 | Flat | 406 | 10.50 ± 0.41 | Li et al. (2017) |
| $TiO_2$-coated carbon membrane | 440 (carbon) | 32.6 | | | 0.0015 | Tube | 401.3 | 9 | Yang et al. (2011) |
| $TiO_2$-coated carbon membrane | 400 (carbon) | 32.6 (carbon) | | | 0.0015 | Tube | | 9 | Yang et al. (2012) |
| $TiO_2$-coated carbon membrane | 410 | 32.6 | | | 0.0017 | Tube | | | Wang et al. (2014) |
| $TiO_2$-coated carbon membrane | 410 | 41.2 | | | 0.0009 | Flat | | 2.2 | Liu et al. (2016a,b) |
| Ebonex® ($TiO_x$) membrane | Bimodal: less than 10 nm and 1000 2000 nm | 30.7 | 2.78 | 391 | 0.0096 (outer) 0.0023 (inner) | Tube | 49.3 | | Zaky and Chaplin (2013) |
| Ebonex® ($TiO_x$) membrane | Bimodal: less than 10 nm and 1000 2000 nm | 30.7 | 2.78 | 391 | 0.0096 (outer) 0.0023 (inner) | Tube | 49.3 | | Zaky and Chaplin (2014) |
| Electrospun PSU/Electrosprayed $Ti_4O_7$-coated carbon cloth | Bimodal: 15,000 nm 100,000 nm | 80 | | | 0.0010 | Flat cloth | 43,571 | 46 51 | Santos et al. (2016) |
| Reduced $TiO_2$ ($TiO_x$) UF membrane | 2990 | 30.4 | 0.66 | | 0.0016 (inner) 0.0032 (outer) | Tube | 3208 | 11.32 | Guo et al. (2016a,b) |
| $Ti_4O_7/Al_2O_3$ near UF membrane | 200-300 ($Ti_4O_7$) | | | | 0.0063 (inner) 0.0110 (outer) | Layer of $Ti_4O_7$ deposited on inner surface $Al_2O_3$ tube | 1019 (with $Ti_4O_7$ layer) | 200 | Geng and Chen (2016) |
| $Ti_4O_7/Al_2O_3$ near UF membrane | 200-300 ($Ti_4O_7$) | | | | 0.0063 (inner) 0.0110 (outer) | Layer of $Ti_4O_7$ deposited on inner surface $Al_2O_3$ tube | 1019 (with $Ti_4O_7$ layer) | 200 | Geng and Chen (2017) |
| $RuO_2$-coated Ti membrane | 980 | 27 | 0.0195 | | | Tube | | | Zhang et al. (2016) |
| $Ti_5O_9/Ti_4O_7$ MF membrane | 1400 nm median pore size | 42 | 0.4 | 8.48 | 0.0017 (inner) 0.0032 (outer) | Tube | 3300 | | Trellu et al. (2018) |

**Table 2**
Recapitulative table of operating conditions of REMs used as anode for electro-oxidation of organic pollutants.

| Anode (working electrode) | Cathode | Pollutant (Conc., mgC $L^{-1}$) | Current density (mA $cm^{-2}$) Cell potential (V) Anode potential (V) | Permeate flux ($L\ h^{-1}\ m^{-2}$) | Electrolyte (mM) | Reference |
|---|---|---|---|---|---|---|
| Porous Carbon | SS | Phenol (344 2375) | 54 61 | | NaCl (2050) | Korbahti and Tanyolac (2003) |
| CNT/carbon felt | CNT/carbon felt | Red X-3B (18.5) | 10 | 1700 | $Na_2SO_4$ (21) | Yang et al. (2009) |
| CNT/PTFE filter | SS | Methylene blue (1.3)<br>Methyl orange (4.2) | 1 3 | 52 | NaCl (10 100) | Vecitis et al. (2011) |
| CNT, Sb-doped $SnO_2$-coated CNT, surface-treated CNT /PTFE filters | SS | Methyl Orange (168)<br>Methylene Blue (192)<br>Phenol (72)<br>CTAB (24)<br>Methanol (12)<br>Formaldéhyde (12)<br>Formate (12) | 0.1 1.7<br>1 3<br>0.4 1.8 (vs. Ag/AgCl) | 52 | $Na_2SO_4$ (100) | Gao and Vecitis (2011) |
| CNT, $SnO_2$-coated CNT, Sb-doped $SnO_2$-coated CNT, Bi-doped $SnO_2$-coated /PTFE filters | SS | Oxalate (100)<br>Ethanol (7)<br>Methanol (5)<br>Formaldehyde (11)<br>Formate (20) | 0.1 3.5<br>1.8 6<br>0.7 3.0 (vs. Ag/AgCl) | 52 104 | $Na_2SO_4$ (10) | Liu et al. (2013) |
| CNT/PTFE filter | SS | Phenol (72) | 0.8 2.1 (vs. Ag/AgCl) | 55 | $Na_2SO_4$ (100) | Gao and Vecitis (2012b) |
| CNT, B-doped CNT, N-doped CNT PTFE filters | SS | Phenol (14 72) | 0.1 1.5<br>1 3<br>0.4 1.6 (vs. Ag/AgCl) | 52 | $Na_2SO_4$ (100) | Gao and Vecitis (2012a) |
| CNT/PTFE filter | SS | Methylene blue (1.3 223)<br>Methyl orange (4.2 924) | 0.1 1.7<br>1 3<br>0.4 1.4 (vs. Ag/AgCl) | 52 | NaCl (10) | Liu and Vecitis (2012) |
| CNT/PTFE filter | Ti or CNT | $Fe(CN)_6^4$ (12 180) | 0.0 0.7 (vs. Ag/AgCl) | 7 140 | $Na_2SO_4$ (1 100) | Schnoor and Vecitis (2013) |
| CNT/PTFE filter | SS | Phenol (72) | 2 3.5<br>0.8 2.1 (vs. Ag/AgCl) | 55 | $Na_2SO_4$ (100) | Gao and Vecitis (2013) |
| Graphene nanoplatelets: CNT/PTFE filter | SS | $Fe(CN)_6^4$ (6 120)<br>Tetracycline (26)<br>Phenol (38)<br>Oxalate (13) | 0 20<br>0 3<br>0 1 (vs. Ag/AgCl) | 52 | $Na_2SO_4$ (10) | Liu et al. (2014) |
| CNT/PTFE filter combined with CNT-PVDF membrane | CNT/PTFE filter combined with CNT-PVDF membrane | Nitrobenzene (7.2)<br>Aniline (7.2) | 0 4 | 55 | $Na_2SO_4$ (10) | Gao et al. (2014) |
| CNT surface-treated CNT /PTFE filter | SS | Phenol (72)<br>Oxalate (120)<br>$Fe(CN)_6^4$ (12)<br>Ascorbate (72) | 0 2.3 (vs. Ag/AgCl) | 55 | $Na_2SO_4$ (100) | Gao et al. (2015a,b) |
| CNT/PTFE filter | Ti or CNT | Tetracycline (53)<br>Synthetic and real spiked effluent | 0 3<br>0 1 (vs. Ag/AgCl) | 52 | $Na_2SO_4$ (10) | Liu et al. (2015) |
| | Pt | | 2.5 12.5 | 300 | | Liu et al. (2016a,b) |

**Table 2** (*continued*)

| Anode (working electrode) | Cathode | Pollutant (Conc., mgC L $^{1}$) | Current density (mA cm $^{2}$) Cell potential (V) Anode potential (V) | Permeate flux (L h $^{1}$ m $^{2}$) | Electrolyte (mM) | Reference |
|---|---|---|---|---|---|---|
| Carbon aerogel, $SnO_2$-coated carbon aerogel, Sb-doped $SnO_2$-coated carbon aerogel | | Tetracycline (30) | | | $Na_2SO_4$ (69) | |
| CNT, carboxylated CNT /PTFE filters | SS | Ibuprofen (0.7 15) | 0.1 0.4<br>0 3 | 12.8 128 | NaCl (10)<br>HCl (10) | Bakr and Rahaman (2016) |
| Polyaniline-coated CNT/PVA filter | Ti | Methylene blue (3) | 0.17<br>3 | 20 | Nothing or $Na_2SO_4$ (10) | Duan et al. (2016) |
| Sb-doped $SnO_2$-coated coal-based carbon | SS | Tetracycline (30) | 0 4 | 150 | $Na_2SO_4$ (100) | Liu et al. (2017) |
| $Fe^0$ NP doped CNT/PTFE filter | Pt | Metoprolol (1.3) | 0.5 1 (vs. Ag/AgCl) | 40 | | Yanez et al. (2017) |
| CNT, B-doped CNT /PTFE filters | SS | Bisphenol A (0.8 80) | 0.1 6<br>0 3 | 32 128 | NaCl (0 100) | Bakr and Rahaman (2017) |
| CNF/PES forward osmosis membrane | Ti | Phenol (360) | 0 3 | 5 15 | $Na_2SO_4$ (1000) | Li et al. (2017) |
| $TiO_2$-coated carbon membrane | SS | Diesel fuel/Tween 80 (200 mg L $^{1}$) | 0.67<br>2 | 80 | $Na_2SO_4$ (104) | Yang et al. (2011) |
| $TiO_2$-coated carbon membrane | SS | Diesle fuel/Tween 80 (200 1000 mg L $^{1}$) | 0.67<br>2 | | $Na_2SO_4$ (104) | Yang et al. (2012) |
| $TiO_2$-coated carbon membrane | SS | Phenol (144 720) | 0.3 | 112 971 | $Na_2SO_4$ (104) | Wang et al. (2014) |
| $TiO_2$-coated carbon membrane | SS | Tetracycline (30 150) | 0.5 2.5 | | $Na_2SO_4$ (104) | Liu et al. (2016a,b) |
| Ebonex® ($TiO_x$) membrane | SS | $Fe(CN)^6_4$ (60)<br>p-methoxyphenol (84)<br>Oxalic acid (120) | 0 3.5<br>0 3 (vs. SHE) | 15 80 | $NaClO_4$ (10) | Zaky and Chaplin (2013) |
| Ebonex® ($TiO_x$) membrane | SS | p-methoxyphenol (84)<br>p-nitrophenol (72)<br>p-benzoquinone (72) | 0 3.5<br>0 3 (vs. SHE) | 35 55 | $NaClO_4$ (10) | Zaky and Chaplin (2014) |
| Electrospun PSU/ Electrosprayed $Ti_4O_7$-coated carbon cloth | BDD | Phenol (72) | 1 | 6100 | $K_2HPO_4$ (100) | Santos et al. (2016) |
| Reduced $TiO_2$ ($TiO_x$) UF membranes | SS | $Fe(CN)^4_6$ (60)<br>Oxalic acid (24)<br>Coumarin (108)<br>Terephthalic acid (9.2) | 0 3.14 (vs. SHE) | 50 1500 | $K_2HPO_4$ (100)<br>$NaClO_4$ (100) | Guo et al. (2016b) |
| $RuO_2$-coated Ti membrane | SS | Tricyclazole (11 57) | 3 20 | 417 | $Na_2SO_4$ (35) | Zhang et al. (2016) |
| $Ti_5O_9/Ti_4O_7$ MF membrane | SS | Oxalic acid (18 870)<br>Paracetamol (9 220)<br>Phenol (18 140) | 6 30<br>4 6.5 | 100 3000 | $Na_2SO_4$ (50) | Trellu et al. (2018) |

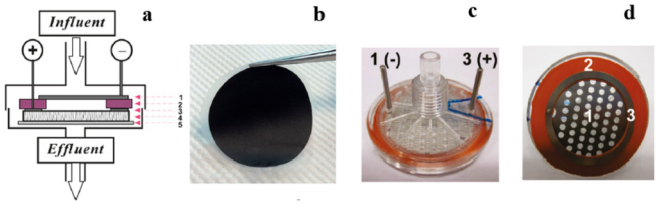


**Fig. 1.** (a) Schematic of an electrochemical CNT filtration system consisting of (1) a perforated titanium shim cathode, (2) an insulating silicone rubber separator and seal, (3) a titanium anodic ring, (4) a CNT anodic filter, and (5) a PTFE membrane support and (b) image of the CNT anodic filter, and (c, d) images of the modified filtration casing. Adapted with permission from Liu et al. (2014) and Vecitis et al. (2011).

Donaghue and Chaplin, 2013). Most treatment systems are therefore operated under mass transport limited conditions, where reaction rates are governed by the diffusion of contaminants to the electrode surface. Therefore, current research is focused on the development of high electroactive surface area electrodes that utilize strategies to maximize mass transport rates (Guo et al., 2016b; Nayak and Chaplin, 2018).

The use of high surface area 3D electrodes in parallel plate configurations only result in a small increase in reaction rates, as features of electrode roughness are smaller than the diffusion length and therefore become averaged into the diffusion field (Bard and Faulkner, 2000). However, REMs have the advantage of having a high specific surface area available for electrochemical reactions (Zaky and Chaplin, 2013; Guo et al., 2016b), due to the convection enhanced transport of dissolved species and the very small pore diameters that allow for fast radial mass transport inside the pores (Liu and Vecitis, 2012; Zaky and Chaplin, 2013; Guo et al., 2016b). The electrode's porous structure, electrical conductivity, and whether the reaction is limited by charge or mass transfer will all affect the electroactive surface area available for reaction (Alkire and Gracon, 1975; Trainham and Newman, 1977a,b, 1978; Lasia, 1997).

The total electroactive surface area available for reaction using REMs was estimated by electrochemical impedance spectroscopy (EIS) and cyclic voltammetry (CV) methods under flow through conditions (Zaky and Chaplin, 2013; Guo et al., 2016a, 2016b; Jing and Chaplin, 2016). These methods rely on measuring the charging current and calculating the double layer capacitance ($C_{dl}$), which can be converted to an electroactive surface area estimate by assuming a value for the specific capacitance (i.e., F $cm^{-2}$). For metal oxide electrodes values of 10–100 μF/$cm^{-2}$ were proposed (Antropov, 1972). Calculation of the electroactive surface area by these methods provides an upper bound estimate, which is indicative of the surface area assessable to the supporting electrolyte and available for electrode charging. Comparing these estimates to the total surface area of REMs measured by Hg porosimetry, indicated that only a fraction of the total surface area of the REMs were electroactive (i.e., 1.5–11.4%) (Zaky and Chaplin, 2013; Guo et al., 2016b; Jing et al., 2016). Roughness factors were also calculated at values between 111 and 1227, which were determined as the ratio of the measured electroactive surface area to that of the nominal projected surface area (Zaky and Chaplin, 2013; Guo et al., 2016a, 2016b; Jing et al., 2016). There are two probable explanations for the low fraction of electroactive surface to total surface area. The first is related to electrode conductivity. If the electrode conductivity is low, then there can be a significant potential drop in the electrode phase, resulting in only a fraction of the total surface area being measured. The second explanation is related to a large portion of the surface area being inaccessible to the electrolyte. In this case the flowing electrolyte cannot enter all of the pores either due to size exclusion or a lack of interconnectivity of the pores (Zaky and Chaplin, 2013). In either case, these scenarios show the importance of synthesizing electrodes with a high conductivity and interconnectivity of the fluid transport pores. Engineering of the porous REM structure has received little attention and is an important area for future research.

The total electroactive surface area measured by EIS and CV methods is the maximum possible area available for reaction, and the actual surface area that participates in reaction depends on whether the reaction of interest is limited by charge or mass transfer (Trainham and Newman, 1977a,b, 1978; Lasia, 1997). Under the condition of charge transfer control, the potential drops drastically with distance from the counter electrode (or depth into the REM). This condition was investigated rigorously in porous electrodes assuming Butler Volmer kinetics, and numerical simulations indicated that the potential drop is a function of the electrolyte and electrode conductivity, specific surface area, counter electrode placement, and kinetic parameters (i.e., exchange current density, electron transfer coefficient) (Trainham and Newman, 1977a,b, 1978; Lasia, 2008). For facile reaction kinetics the potential may drop significantly and since the current is exponentially related to the potential (according to Butler Volmer kinetics) reactions are restricted primarily to the surface closest to the counter electrode (Trainham and Newman, 1977a,b, 1978; Lasia, 2008). Under this situation the reactive surface area is significantly less than the total electroactive surface area.

Under conditions of mass transport control and negligible potential drop in the electrode phase, the concentration and potential profiles with depth into the REM can be calculated analytically (Fedkiw, 1981). The concentration profile (C(y)) follows an exponential decrease with distance into the REM, according to Eq. (5).

$$\frac{C(y)}{C_F} \quad exp\left( \quad aL\frac{k_m}{J}\frac{y}{L}\right) \tag{5}$$

where $k_m$ is the mass transfer coefficient (m/s), $a$ is the specific surface area ($m^{-1}$), $J$ is the REM flux (m/s), $L$ is the REM thickness, $C_F$ is the feed concentration (mol $m^{-3}$), and $y$ is the distance into the REM.

Under mass transport control the reactive surface area can reach that of the electroactive surface area and is dependent on mass transport parameters (i.e., $k_m$, $J$). The potential drop with depth into the REM is typically approximately linear and since under mass transport control the current is no longer an exponential function of potential the entire REM thickness can be utilized for reaction. However, the above analysis only applies for thin REMs, as the potential drop in solution can be significant for thick REMs and eventually lead to charge transfer limitations. Therefore, further studies are required for developing counter measures such as additional current feeders or improvement of the reactor design. One such approach would be a design that utilizes a stack of thin REMs, each separated by a thin gasket. A stack of thin, alternating anodes and cathodes would allow for sequential oxidative/reductive electrochemistry, a high utilization of the surface area, and minimal potential losses due to solution resistance.

In general there has been little attention dedicated to understanding reactive transport in REMs. However, there is a large body of literature available for packed bed flow through electrodes that are applicable to REMs (Trainham and Newman, 1977a,b, 1978; Fedkiw, 1981; Risch and Newman, 1984). This type of analysis can greatly enhance REM development and optimization and is a critical area for future study.

## 4. Convection-enhanced mass transport of organic pollutants

For the analysis of AO of organic pollutants using conventional

2D electrodes, the most widely used approach is to consider that the electro oxidation takes place either under mass transfer limi tations or under charge transfer limitations (Comninellis et al., 2008; Panizza and Cerisola, 2009). The mass transfer limit can be estimated from the limiting current density ($i_{lim}$, Eq. (6)), which is related to the mass transfer rate constant and concentration of organic compounds (Panizza et al., 2001; Rodrigo et al., 2001; Comninellis et al., 2008).

$$i_{lim}(t) \quad 4Fk_mCOD_t \tag{6}$$

In Eq. (6), $i_{lim}(t)$ is the limiting current density (A $m^{-2}$) at time $t$, 4 is the number of electrons exchanged from $O_2$, $F$ is the Faraday constant, $k_m$ is the mass transfer rate constant (m $s^{-1}$) and $COD_t$ is the chemical oxygen demand (mol $m^{-3}$) at time $t$. A mixed kinetic regime can also exist, particularly when strong, stable oxidant species are generated that are transported to the bulk solution (e.g. chlorine, ozone, persulfate) (Martínez Huitle and Ferro, 2006; Panizza and Cerisola, 2009; Martínez Huitle et al., 2015).

At currents above $i_{lim}$, electro oxidation occurs under mass transfer control and the current efficiency strongly decreases with increases in current (Panizza and Cerisola, 2009). This often com promises the energetic sustainability of the AO process for the treatment of low concentration pollutants. Mass transfer limita tions can be reduced by (i) coupling electro oxidation with a pre concentration step (Ganiyu et al., 2015), (ii) continuously adjust ing the current density to the limiting current density during treatment (Panizza et al., 2008), and (iii) improving the fluid dy namics in the electrochemical cell in order to increase the mass transfer rate (Vecitis et al., 2011; Zaky and Chaplin, 2013; Martínez Huitle et al., 2015).

Using conventional plate electrodes in a batch cell, stirring conditions are one of the most crucial parameter for AO efficiency (de Oliveira et al., 2011). Continuous systems such as flow by re actors are more suitable for improving hydrodynamic conditions and for implementation of large scale electrochemical cells (Panizza et al., 2007; dos Santos et al., 2014; Martínez Huitle et al., 2015). Mass transfer processes over a flat plate or in a pipe are often analyzed by nondimensional groups, including the Sherwood number (*Sh*, Eq. (7), ratio between convective and diffusive mass transport) the Reynolds number (*Re*, Eq. (8), ratio of inertia to viscous forces), and the Schmidt number (*Sc*, Eq. (9), ratio of vis cosity to diffusivity) as well as a nondimensional shape factor (*Le*), which depends on the geometry of the electrochemical cell. Values for $k_m$ can be estimated by using correlations, typically under the form of Eq. (10) (Canizares et al., 2006).

$$\text{Sh} \quad \frac{k_m d}{D} \tag{7}$$

$$\text{Re} \quad \frac{ud}{\nu} \tag{8}$$

$$\text{Sc} \quad \frac{\nu}{D} \tag{9}$$

$$\text{Sh} \quad \frac{k_m d}{D} \quad aRe^b Sc^c Le^d \tag{10}$$

In the equations above, $d$ is the characteristic length of the system, $D$ the diffusion coefficient of the organic compound in water, $u$ the fluid velocity, $\nu$ the kinematic viscosity of the fluid and $a$, $b$, $c$, $d$ are constants that are determined empirically. Maximum $k_m$ values that can be achieved are often on the order of $10^{-6}$ – $10^{-5}$ m $s^{-1}$ (Canizares et al., 2006). For example, Zaky and Chaplin (2013) determined a diffusion limited mass transfer rate at the surface of an anode under the form of a pipe as $4.32 \times 10^{-6}$ m $s^{-1}$ (Re 1270; inner diameter and length of the electrode was 1.7 cm and 20 cm, respectively).

One of the main issues of using conventional plate electrodes is the limitation of mass transport through the external diffusion boundary layer film ($\delta_b$). The steady state $\delta_b$ in flow by electro chemical cells can be as high as 100 μm, according to the cross flow velocity and the channel spacing. Thus, the efficiency of the process relies on the diffusion of contaminants through this layer. In this configuration, the use of high surface area electrodes only slightly increases $k_m$ values because the features of electrode roughness are smaller than the diffusion length. Therefore, implementation of porous electrodes in a flow through configuration is the most promising way to overcome diffusion limitations. Using REMs in flow through mode lead to a convective increase of $k_m$, according to the steady state balance between forward convection and diffusion (Liu and Vecitis, 2012). At high flow rates, $\delta_b$ can reach a theoretical length of less than the electrode pore radius. This type of analysis assumes straight, cylindrical pores, where the time scale of diffu sion ($t_D$) (Eq. (11)) and convection ($t_C$) (Eq. (12)) can be estimated.

$$t_D \quad \frac{r_p^2}{D} \tag{11}$$

$$t_C \quad \frac{l}{v} \tag{12}$$

In the equations above, $r_p$ is the average pore radius (m), $D$ is the diffusion coefficient of the organic compound (m $s^{-1}$), $l$ is the electroactive thickness, and $v$ is the average pore velocity (m $s^{-1}$). Using $TiO_x$ REM ($r_p$ 0.85 μm, $l$ 880 μm) for electro oxidation of $Fe(CN)_6^{4-}$, it was reported that diffusion limitation ($t_D > t_C$) would only occur at $J > 1.3 \times 10^6$ L $m^{-2}$ $h^{-1}$ (Zaky and Chaplin, 2013), which is much higher than normal operating conditions of micro filtration membranes. The smaller the electrode pore size, the lower $t_D$ and the lower the diffusion limitations. However, small pore size also strongly increases pressure drops across the REM and the permeability (in terms of L $h^{-1}$ $m^{-2}$ $bar^{-1}$) of REM decreases. This means that higher transmembrane pressure has to be invoked as a driving force for increasing the permeate flux (i.e. the con vection rate). This is the reason why the performances of an ul trafiltration $TiO_x$ REM (3200 L $h^{-1}$ $m^{-2}$ $bar^{-1}$) surpassed those of Ebonex® electrodes (50–70 L $h^{-1}$ $m^{-2}$ $bar^{-1}$), which was not tailored for water treatment (Zaky and Chaplin, 2013; Guo et al., 2016b). Besides, one of the main advantages of using CNT REMs is the possibility to generate a thin filtration layer (41 μm) with low pore size (115 nm) and high porosity (85%), leading to a perme ability in the range 500–2000 L $h^{-1}$ $m^{-2}$ $bar^{-1}$ (Liu and Vecitis,

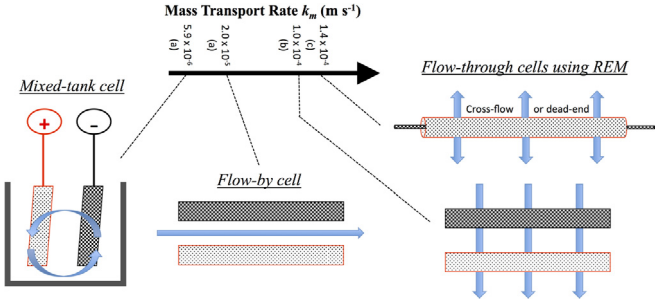


**Fig. 2.** Mass transport rate ($k_m$) reported in the literature according to the electro-chemical cell configuration. In the bottom left, evolution of the diffusion boundary layer ($\delta_b$) in batch and flow-through configurations. (a) dos Santos et al. (2014), (b) Schnoor and Vecitis (2013), (c) Guo et al. (2016b).

2012). Thus, Vecitis et al. (2011) reported a diffusion and convection characteristic time of 3.3 μs and 1.2 s, respectively, for the electro oxidation of a dye molecule in a CNT/PTFE REM.

However, since actual electrode pores are not completely straight and cylindrical, $\delta_b$ will be larger in experimental setups. A good approximation of $k_m$ as a function of the pore fluid velocity is given by Eq. (13).

$$\frac{\varepsilon k_m}{aD} \quad m_1 \left(\frac{v}{aD}\right)^{1/3} \tag{13}$$

where $\varepsilon$ is the REM porosity, $a$ is the specific surface area ($m^{-1}$), and $m_1$ is an experimentally determined constant. This correlation was applied to numerous packed bed electrodes and they should also be applicable to REMs (Wilson and Geankoplis, 1966).

Fig. 2 shows different values of $k_m$ reported in the literature according to the electrochemical cell configuration (batch, flow by, and flow through). Operation of AO under convective limited conditions is a great advantage; since $k_m$ can be simply increased by performing electro oxidation at a higher permeate flux. While Yang et al. (2009) reported a 1.6 fold improvement of $k_m$ using a flow through configuration, Liu and Vecitis (2012) showed an in crease of the mass transfer limited current density from 0.97 (in batch) to 6.1 mA $cm^{-2}$. Even better, the study of Guo et al. (2016b) reported a convection enhanced $k_m$ for $Fe(CN)_6^{4-}$ of $1.4 \times 10^{-4}$ m $s^{-1}$, close to the estimated charge transfer limit. Thus, for the treatment of low concentrations of organic compounds, the current efficiency can be improved simply by increasing the permeate flux (i.e. the convection rate). For example, the current efficiency for the removal of oxalic acid (TOC 24 mg $L^{-1}$) by $TiO_x$ REM increased from 25% to 84% at 90 and 561 L $h^{-1}$ $m^{-2}$, respec tively (Fig. 3). Guo et al. (2016b) proposed a semi empirical analysis of reaction kinetics in REMs for the determination of the observed rate constant ($k_{obs}$). It takes into account reaction ($k_r$), diffusion ($k_d$) and convection ($k_c$) rate constants (Eq. (14), (15)). This approach highlights that the decrease of the diffusion limitations can create a new challenge: increasing the reactivity of REMs ($k_r$) in order to take advantage of the convection enhanced mass transfer in flow through electrochemical cells.

$$k_{obs} \quad \left(\frac{C_{in} \quad C_{out}}{C_{in}}\right) k_C \quad \frac{k_c}{1 + \frac{k_c}{k_i}} \tag{14}$$

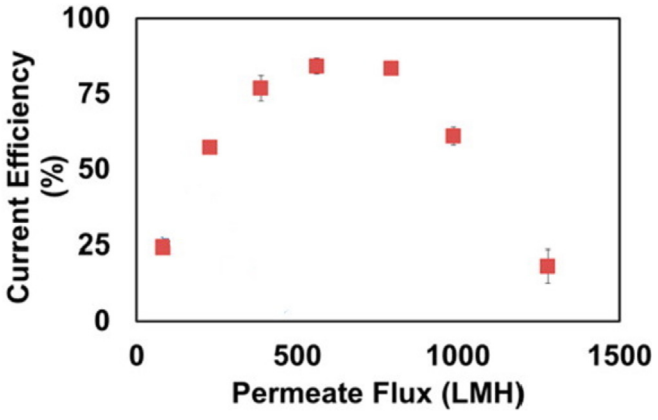


**Fig. 3.** Current efficiency for the oxidation of 1 mM oxalic acid as a function of permeate flux by using ultrafiltration $Ti_4O_7$ REM. Experimental conditions: T 21 °C; Anode potential 2.94 V *vs.* SHE; Electrolyte 100 mM $NaClO_4$. Reprinted from Guo et al. (2016b).

$$k_C \quad J \quad \frac{Q}{A} \tag{15}$$

where, $C_{in}$ and $C_{out}$ are the concentration of organic compounds in the influent and effluent of the REM, respectively, $Q$ is the permeate flux ($m^3$ $s^{-1}$), $A$ is the geometric surface area of the REM ($m^2$), $k_c$ is the convection rate constant (m $s^{-1}$) and $k_i$ (m $s^{-1}$) represents either $k_d$ (diffusion rate constant) or $k_r$ (kinetic rate constant) ac cording to the limiting process.

Organic compound adsorption is another important parameter to consider during REM operation, particularly when using CNTs (Vecitis et al., 2011; Liu and Vecitis, 2012; Liu et al., 2015). Adsorption can increase the effective residence time of target pol lutants within the electroactive pore structure. For example, the differences in electro oxidation efficiency of oxalate, formate, formaldehyde and alcohols were reported to be attributed to different sorption kinetics (Liu et al., 2013). Thus, a strategy for enhanced performance is to tailor the electrode surface chemistry for strong adsorption of organic pollutants (Gao and Vecitis, 2011; Liu et al., 2013; Gao et al., 2015a). However, adverse effects can also arise from adsorption. For example, reactive site saturation by adsorbed tetracycline was observed to limit the overall electro oxidation kinetics (Liu et al., 2015).

## 5. Charge transfer and oxidation mechanisms

Apart from the high electroactive surface area and convection enhanced mass transport, the efficiency of AO depends on the reactivity of the REM. The choice of both the electrode material and operating conditions strongly influences charge transfer mecha nisms. Table 2 summarizes operating conditions reported in studies investigating the AO of organic pollutants using REMs. The studies on $TiO_2$ coated carbon membranes were also included in Table 2, as these materials can also form •OH under anodic polarizations (Wang et al., 2014). The process is similar to the well known pho tocatalytic process, but the nature of the energy input is different.

### 5.1. Oxygen evolution potential

Anode materials used for AO are often divided into two main classes according to their OEP (Fig. 4): (i) "active" electrodes with low overpotential for OER (<0.3/0.4) and (ii) "non active" elec trodes with high overpotential for OER (>0.4) (Panizza and Cerisola, 2009; Martínez Huitle et al., 2015). Only non active electrodes are able to generate large quantities of •OH from water oxidation ($E^\circ$ 2.38 V *vs.* SHE) that are physisorbed at the electrode surface and are readily available for oxidation of organic compounds. The production of other oxidant species such as ozone ($E^\circ$ 1.51 V *vs.* SHE) or sulfate radicals ($E^\circ$ 2.4 V *vs.* SHE) is also possible (Martínez Huitle et al., 2015). Anode materials can also be classified according to their selectivity for •OH, $H_2O_2$, or $O_2$ evolution, as analyzed by Siahrostami et al. (2017). Thermodynamically, the

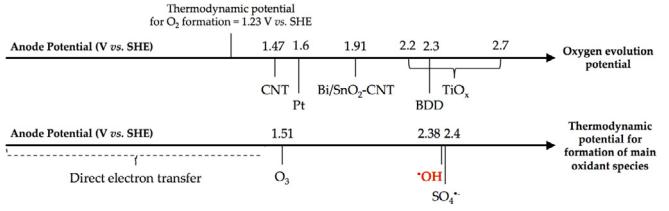


**Fig. 4.** Oxygen evolution potential of various electrode materials used as REM (CNT, Bi/$SnO_2$-CNT, $TiO_x$) and thermodynamic potential for formation of main oxidant species. Higher oxygen evolution potential favors the formation of oxidant species.

selectivity of an anode material for the formation of •OH from water oxidation depends on the free energy of the adsorbed •OH. If the free energy of the adsorbed •OH is comparable to that of the aqueous phase •OH, then it will desorb from the anode surface and be available for reaction. Conversely, if the free energy of the adsorbed •OH is significantly lower than the aqueous phase •OH, it will not desorb and will react to form $O_2$ or $H_2O_2$ (Siahrostami et al., 2017). In addition, the OER can also affect the electrocatalytic activity of the material due to oxygen bubbles blocking reactive sites (Liu et al., 2013). These oxygen bubbles, as well as $H_2$ production at the cathode, were reported to increase pressure drop across the REM due to the decrease of the active filtration area (Trellu et al., 2018).

#### 5.1.1. CNT based REMs

One of the most widely used material as REM is carbon, which is considered as an "active" electrode. For example, an OEP of 1.7 V *vs.* SHE was reported for activated carbon fibers (Fan et al., 2008). At low potential, electro oxidation of organic compounds is possible by direct electron transfer reactions that are dictated by the electrocatalytic activity of the material (Panizza and Cerisola, 2009). However, some organic compounds are recalcitrant to direct electron transfer (e.g. *p* benzoquinone), thus leading to incomplete oxidation. Moreover, electropolymerization can also occur (Belhadj Tahar and Savall, 2009a, 2009b) and adsorption of polymers at the anode surface leads to a strong decrease of the electrocatalytic activity of the material (Panizza and Cerisola, 2009). This issue is of paramount importance when using REMs in filtration mode, since it can also lead to membrane fouling and increased pressure drop across the membrane (Gao and Vecitis, 2012a, 2013; Zaky and Chaplin, 2013, 2014; Trellu et al., 2018). This phenomenon was clearly highlighted by Gao and Vecitis (2012b), who observed CNTs coated by polyphenols and polyphenylene oxides, which were generated from phenol electropolymerization along the entire depth of the CNT layer (~40 μm). A greater amount of phenol removal was observed at anode potential of 0.82 and 1.6 V *vs.* Ag/AgCl, compared to 2.1 V *vs.* Ag/AgCl. Low anode potentials favored electropolymerization of phenols and allowed a physical separation (by adsorption on the electrode surface) of electro generated polymers (Trellu et al., 2018). However, this process is not a long term sustainable method for the removal of organic compounds such as phenol, because of the difficulty in removing polymers from membrane pores (Gao and Vecitis, 2013). Thus, it is necessary to operate REMs at higher anode potential, in the potential region of water oxidation, in order to be able to achieve aromatic ring opening. However, when high anode potentials are required for the complete oxidation of complex molecules, carbon materials suffer from a decrease in current efficiency (due to the OER) and significant electrode corrosion (Liu et al., 2013). For this reason, CNT doping was the focus of several studies, with the aim of increasing both the overpotential for OER and the stability of the electrode. For example, Gao and Vecitis (2012a) demonstrated that boron doped CNTs were able to reduce the extent of electropolymerization, because of the higher work function (i.e. the energy difference between the material Fermi level and the vacuum level) that enhanced the number of electrons transferred for phenol oxidation. Opposite results were obtained by using nitrogen doped CNTs, i.e. lower work function and electropolymerization enhancement. Another strategy that was utilized involved the coating of CNTs with a material possessing a high conductivity and overpotential for the OER. Liu et al. (2013) fabricated Bi doped $SnO_2$–coated CNTs, and similar materials were also synthesized by replacing Bi with Sb. However, using Sb is of less interest for water treatment applications because of the toxicity of Sb. The OEP was increased from 1.27 V *vs.* Ag/AgCl for the uncoated CNT anode to 1.71 V *vs.* Ag/AgCl for the Bi doped $SnO_2$–coated CNT (Liu et al., 2013). Moreover, the Tafel slope of this material was 1.05 V $dec^{-1}$, which is higher than those measured on BDD (0.29 V $dec^{-1}$) (Zhao et al., 2010), indicating relatively slow OER kinetics. Thus, a 2–8 fold increase of the mineralization kinetics for oxalate and other organic compounds, such as ethanol, methanol, formaldehyde and formate were observed.

#### 5.1.2. Magnéli phase based REMs

Studies on the use of $TiO_x$ materials showed the most promising results on the possibility of using a REM for high yields of •OH formation. The OEP reported in the literature for $TiO_x$ materials (mainly $Ti_4O_7$) ranged between 2.2 and 2.7 V *vs.* SHE (Graves et al., 1991; Grimm et al., 1998; Kolbrecka and Przyluski, 1994; Miller Folk et al., 1989), similarly to the widely used (but expensive) BDD anode (2.3 V *vs.* SHE). Guo et al. (2016b) demonstrated the formation of •OH by studying the degradation of organic compounds used as •OH probes. A strong enhancement of the conversion of these •OH probes were observed when increasing the anode potential from 2.14 to 2.64 V *vs.* SHE. Such degradation mechanisms indicated the production of •OH and the anode potential required is consistent with the thermodynamic potential for •OH formation. Thus, high anode potential can be used in order to avoid electropolymerization and to degrade refractory organic compounds by •OH mediated oxidation.

### 5.2. Permeate flux, hydraulic residence time and charge transfer limitation

Different operating conditions can also affect the electro oxidation efficiency. First, the permeate flux and the hydraulic residence time are crucial parameters because of mass transport considerations and reaction time, as discussed in section 3. Increasing the permeate flux too much may also favor the OER by sweeping gas bubbles from the REM surface and enhancing the OER (Guo et al., 2016b; Trellu et al., 2018). This mechanism was attributed to lower removal rates and current efficiencies at high flow rates (Fig. 3) (Guo et al., 2016b; Trellu et al., 2018). In the study of Guo et al. (2016b), the maximum current efficiency for oxalic acid oxidation was 84% at a flux of 561 L $m^{-2}$ $h^{-1}$ using a $Ti_4O_7$ REM and 49% at a flux of 194 L $m^{-2}$ $h^{-1}$ using a $Ti_4O_7$/$Ti_6O_{11}$ REM. The differences arose from the lower reactivity of the $Ti_6O_{11}$ phase. Different optimal values of TOC flux and maximum current efficiency were also achieved according to the current density (Trellu et al., 2018). Thus, the kinetic rate constant ($k_r$) of a REM is an important parameter to consider. This charge transfer limit is governed by the electron transfer rate and by chemical reaction kinetics between organic compounds and electrochemically produced oxidants. Using $Fe(CN)_6^{4-}$ as a model compound, this kinetic limit was calculated to be $1.64 \times 10^{-4}$ m $s^{-1}$ by using an ultrafiltration $TiO_x$ electrode (Guo et al., 2016b), while Schnoor and Vecitis (2013) reported $k_r$ $1.0 \times 10^{-4}$ m $s^{-1}$ using a CNT REM.

### 5.3. Influence of anodic potential distribution within the REM

The potential drop according to the electrode depth in the REM can also influence oxidation mechanisms. The anode potential is sufficiently high for the formation of •OH only in the top portion of the REM closest to the counter electrode (Jing et al., 2016), as explained in section 2. Therefore, when the TOC flux ($[TOC]_{influent} * J_{permeate}$) is higher than the convective mass transport limit, organic compounds reach a depth into the REM where the potential is too low for significant •OH production and therefore only direct electron transfer reactions occur. This mode of operation can decrease the efficiency of the process because of the electropolymerization

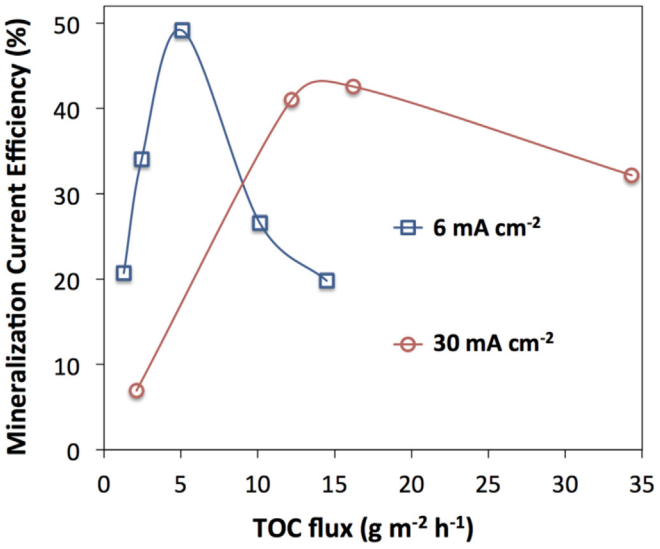


**Fig. 5.** Current efficiency for the oxidation of paracetamol as a function of permeate flux by using $TiO_x$ REM. Experimental conditions: constant permeate flux (150 L h $^{1}$ m $^{2}$); increasing paracetamol concentration (TOC 9 220 mg L $^{1}$); i 6 or 30 mA cm $^{2}$; electrolyte 50 mM $Na_2SO_4$. Adapted from Trellu et al. (2018).

phenomena and presence of organic compounds refractory to direct electron transfer reactions (Zaky and Chaplin, 2014; Trellu et al., 2018). In order to avoid such adverse effects, it is necessary to adjust the operating conditions (TOC flux and current density), so that reactions are limited by convective mass transport and organic compounds are degraded close to the REM surface where •OH are generated (Trellu et al., 2018). These mechanisms have to be taken into consideration for optimization of the process. For example, Trellu et al. (2018) reported that a much higher mineralization current efficiency was achieved at 6 mA $cm^{-2}$ compared to 30 mA $cm^{-2}$ for the treatment of a TOC flux of paracetamol of 5 g $m^{-2}$ $h^{-1}$, but the contrary was observed for the treatment of a TOC flux of 15 g $m^{-2}$ $h^{-1}$ (Fig. 5). Increasing the current density was also observed to prevent REM fouling by electropolymerization of phenol (Trellu et al., 2018).

### 5.4. Conductivity and electrolyte concentration/composition

The conductivity and electrolyte concentration/composition of the influent can also strongly influence electro oxidation efficiency and reaction mechanisms. First, the presence of ions such as $Cl^-$ and $SO_4^{2-}$ can lead to the formation of additional strong oxidant species (active chlorine, $SO_4^{\bullet-}$). The formation of these species favors electro oxidation in the bulk solution and was therefore observed to improve the oxidation efficiency in mass transport limited configurations (Martínez Huitle et al., 2015). In contrast to batch reactors, it was observed that a decrease of the ionic strength (from 100 to 1 mM of $Na_2SO_4$) did not significantly increase the charge transfer resistance (Schnoor and Vecitis, 2013). This result was attributed to the flow through configuration and continuous convective renewal of fresh electrolyte to the REM surface, which resulted in a hydrodynamic reduction of the charge transfer resistance (Schnoor and Vecitis, 2013).

### 5.5. Cathode material

The nature of the cathode material was also shown to be an important consideration. For example, the use of a CNT cathode significantly improved charge transfer efficiency by comparison to perforated Ti as cathode materials (Liu et al., 2015; Schnoor and Vecitis, 2013). The total cell potential required for total conversion of 1 mM $Fe(CN)_6^{4-}$ by using CNT as both anode and cathode was 1 V lower than for the electrochemical cell using a Ti cathode. In this two electrode cell, lower cathode potential was required for water electro reduction by using CNT, thus leading to a shift in the potential distribution towards the anode and strongly reducing the energy required for the overall electrochemical process. Besides, the electrochemical cell configuration and cathode material can also be optimized in order to achieve single pass, sequential reduction oxidation of pollutants, as reported for nitrobenzene by Gao et al. (2014).

CNTs were also used in a sandwich membrane stack in order to perform sequentially EF and AO processes (Gao et al., 2015b). The membrane stack consisted of a CNT filter cathode for $H_2O_2$ generation, which contained $COO^-$ functional groups with chelated $Fe^{2+}$ ions that were capable of participating in the Fenton's reaction at neutral pH and that could be electro regenerated, an insulating separator and a CNT filter anode. This study emphasized synergetic effects from the sequential combination of EF and AO in filtration mode, thus constituting an interesting proof of concept of this innovative reactor design. Performing the EF process at neutral pH is a significant advantage, which has been the goal of several heterogeneous catalyst synthesis studies (Banuelos et al., 2013; Ammar et al., 2015; Ganiyu et al., 2017).

## 6. REM lifetime

### 6.1. Fouling

Despite continuous improvements aimed at mitigating fouling in membrane processes, the fouling issue in membrane filtration for water treatment remains the most significant challenge. Fouling is problematic for both ceramic and polymeric membranes, where colloids, macromolecules, and microorganisms are responsible for the formation of fouling layers (Guo et al., 2012). The main fouling mechanisms for microfiltration and ultrafiltration membranes are (i) deposition (cake formation) (Yuan et al., 2002), (ii) pore blockage (Yuan et al., 2002; Costa et al., 2006; Wang and Tarabara, 2008; Guo et al., 2012; Lee et al., 2013; Dilaver et al., 2018) and (iii) adsorption (hydrophobic and electrostatic interactions) (Fan et al., 2001; Lee et al., 2004; Costa et al., 2006; Jung et al., 2006; Yamamura et al., 2007; Xiao et al., 2011; De Angelis and de Cortalezzi, 2013). Particularly, the hydrophobicity of the membrane material is a crucial parameter that often governs fouling (Howe and Clark, 2002; Xiao et al., 2011; Lee et al., 2013; Geng and Chen, 2016). Using several model foulants (i.e., polyethylene glycol, natural humic acid and a mixture of organic and inorganic solutes), comparative studies highlighted that ceramic materials such as $TiO_2$ with higher hydrophilic character (15.6 ± 3.4° water contact angle) than PVDF (69.3 ± 2.9°) were less susceptible to fouling by hydrophobic organic molecules or colloids (Lee et al., 2013). On the contrary, hydrophobicity and $\pi$ $\pi$interactions of CNT filters (contact angle 66.2°) favor strong adsorption of water contaminants, such as aromatic compounds or natural organic matter (Liu and Vecitis, 2012). Because of the lower hydrophobic interactions between organic foulants and ceramic materials, the main fouling mechanism of ceramic membranes is related to initial pore blocking and a fast transition to cake formation, which is primarily removed by a physical cleaning (Guo et al., 2012; Lee et al., 2013; Dilaver et al., 2018). Besides, electrostatic interactions between the membrane and charged compounds have also to be taken into consideration in order to limit membrane fouling and improve the efficiency of physical cleaning of membranes (Lee and Kim, 2014; Zhang and Vecitis, 2014).

Further mechanisms have to be considered when studying REMs (Jing et al., 2016; Ronen et al., 2016; Formoso et al., 2017). The combination of filtration processes with other processes is an important current area of research in order to avoid fouling issues. In particularly, oxidation at the interface combined with enhanced electrostatic repulsive forces of foulants was reported to lead to a non negligible delay in membrane fouling of membrane electro oxidizers (e.g. Alumina Ceraflo membrane) (Ronen et al., 2016; Formoso et al., 2017; Mameda et al., 2017). Coupling membrane and electro oxidation processes provides a promising tool to ensure both the removal of targeted molecules and high throughput *via* the prevention of fouling (Geng and Chen, 2017). Thus, self cleaning electrochemical membrane reactors are ex pected to emerge in the next few years (Yang et al., 2011; Ahmed et al., 2016; Ronen et al., 2016; Formoso et al., 2017).

In electrically enhanced filtration processes, the applied electric field can also increase electrostatic repulsions. For example, Geng and Chen (2016) observed the repulsion of negatively charged molecules (e.g. humic acids) by a $Ti_4O_7/Al_2O_3$ composite under cathode polarization (Huotari et al., 1999; Geng and Chen, 2016, 2017). This phenomenon can be described by the extended Nernst Planck equation (Eq. (16)), which takes into consideration diffusive, migrational, and convective fluxes.

$$J_i \quad D_i\frac{\partial c_i}{\partial_x} \quad D_i c_i \frac{z_i F}{RT}\frac{\partial \phi}{\partial x} + c_i v(x) \tag{16}$$

where $J_i$ is the averaged flux of the charged species i (mol $m^{-2}$ $s^{-1}$), $c_i$ is the concentration in the solution (mol $m^{-3}$), $D_i$ is the diffusion coefficient ($m^2$ $s^{-1}$), $z_i$ is the valence number of the charged species $i$, $F$ is the Faraday constant ($9.648 \times 10^4$ C $mol^{-1}$), $R$ is the ideal gas constant (8.314 J $mol^{-1}$ $K^{-1}$), $T$ is the absolute temperature (K), $\partial\phi/\partial x$ is the electrical field (V $m^{-1}$) and $v(x)$ is the velocity of the fluid through the porous media (m $s^{-1}$).

If the applied electric field reaches a critical value, the combined diffusive and convective fluxes towards the REM (Geng and Chen, 2017) will be balanced by the migrational flux away from the REM. Under conditions where the diffusive flux is negligible compared to convection, the theoretical value for the critical elec tric field strength ($\mathscr{E}_{critical}$) at which the net ion migration velocity towards the REM is zero can be estimated by Eq. (17) (Huotari et al., 1999).

$$\mathscr{E}_{critical} \quad \frac{v(x)}{u_i} \tag{17}$$

where $u_i$ $D_i\frac{z_i F}{RT}$ is the mobility of the charged species.

Electrostatic interactions can also be enhanced between nega tively charged species and the anode, which enhances organic compound adsorption (Liu and Vecitis, 2012; Zhou et al., 2017). Degradation of the adsorbed molecules at the REM surface can prevent the formation of the fouling layer (Ahmed et al., 2016). However, if electro oxidation kinetics is not sufficient to degrade adsorbed molecules, REM fouling can occur by one of the prevailing fouling mechanisms, which is dependent on the solute size and hydrophobicity. For example, the electrochemical filtration of polystyrene (PS) microspheres (1.58 μm) through a $TiO_x$ REM (active layer pore size < 10 nm), resulted in intermediate pore blocking followed by cake layer formation and reduced the access of solutes to the electroactive surface. However, the fouling layer was easily removed using a backwash with either anodic or cathodic potential on the REM (Jing et al., 2016).

Electrochemical processes can also have adverse effects on membrane fouling when electropolymerization of organic com pounds occurs at the surface of anode materials, especially with phenolic compounds, (Belhadj Tahar and Savall, 2009a; Comninellis and Nerini, 1995; Gao and Vecitis, 2013; Yang et al., 2013; Ahmed et al., 2016; Trellu et al., 2018). Phenol polymeriza tion is due to the production of intermediate phenolic free radicals that adsorb on the electrode surface and polymerize by radical chain reaction mechanisms (Comninellis and Pulgarin, 1991; Ferreira et al., 2006; Gao et al., 2015a). The formation of adsorb able recalcitrant polymers inside REM pores can be avoided by using high $O_2$ overpotential anodes such as $TiO_x$ and appropriate operating conditions to achieve the total mineralization of phenolic compounds (Trellu et al., 2018). Another side effect to take into consideration is the precipitation of salts that are present in the electrolyte (Gao and Vecitis, 2012a). In the EF system, ferric ions can also precipitate into $Fe(OH)_3$ at pH values higher than 6. Thus, an optimal pH of 3 has to be maintained in order to avoid the pre cipitation of iron (III) hydroxide at the membrane surface that could greatly affect the flux through the porous electrode (Xu et al., 2016). Such precipitation phenomena can reduce the degradation rate by decreasing the number of active sites for adsorption or reaction and by reducing mass transfer because of lower flux (Li et al., 2016; Zhou et al., 2017). For the treatment of real effluents containing metallic ions, electro deposition on cathodic polarized REMs might also contribute to flux decline.

Bubble flow resistance is also responsible for flux decrease in REMs without any relation to common fouling mechanisms (Geng and Chen, 2017; Trellu et al., 2018). Gas bubbles are generated at the anode surface during water electrolysis when the anode potential exceeds the OEP (Saleh, 2007; Kapałka et al., 2010). They act as a shield and prevent molecules from reaching the reactive surface (Liu et al., 2013; Sun et al., 2013). Electro generated gas bubbles are then swept from the membrane surface by the convective flux (Guo et al., 2016b; Trellu et al., 2018). From another point of view, several studies mentioned that these gas bubbles could be used as a physical barrier to prevent fouling (Ahmed et al., 2016) or increase the electrochemical backwash efficiency by lifting the fouling layer (Wu et al., 2008; Jing et al., 2016; Jing and Chaplin, 2016).

As regards to the fouling issue, it is also important to mention that ceramic membranes used as REMs are robust from a me chanical, thermal and chemical standpoint. These characteristics allow them to withstand harsh cleaning conditions to remove foulants by backwash, solvent or acid base chemical treatment and even polarity reversal (Hayfield, 2001; Gao and Vecitis, 2013; Lee et al., 2013; Dashtban Kenari and Barbeau, 2016; Guo et al., 2016b).

These studies highlighted the potential positive and negative effects occurring during REM operation regarding fouling. How ever, only few studies have been conducted and more work is needed to investigate the ability of REMs to reduce fouling and enhance regeneration in complex real water matrices.

### 6.2. Corrosion

The cathode material is usually less susceptible to corrosion as confirmed by several studies with various electrode materials such as graphite (Ayadi et al., 2013), CNT (Gao et al., 2015a,b), graphene composite (Zhao et al., 2013) and graphite felt on PTFE (Ren et al., 2016). However, using a REM as an anode can cause both passiv ation and corrosion of the material. Therefore, the development of anode materials with high anodic stability is of great importance, in particular for organic compound oxidation processes that require application of relatively high potentials.

Because the standard potential of carbon oxidation reactions is 0.207 V *vs.* SHE (Kinoshita, 1988), corrosion of carbon based REMs is often inevitable at high anode potentials. The oxidation of carbon to $CO_2$ and/or CO leads to the destruction of the carbon electrode. For example, Yi et al. (2015) investigated the mechanisms of

electrochemical degradation of MWCNTs in acidic media. At high anode potential for OER, MWCNTs undergo an electrochemical activation by the formation of oxygenated functional groups, fol lowed by a passivation due to a fully covered oxide layer (Ohmori and Saito, 2012; Tominaga et al., 2014; Yi et al., 2015). Therefore, it is necessary to modify carbon based anodes in order to extend their lifetime. Attempts to increase the resistance to AO of CNTs were centered on anchoring or coating metal nanoparticles ($Co_3O_4$, Bi doped $SnO_2$) at their surface (Liu et al., 2013; Lu and Zhao, 2013). Results demonstrated an increase of the stability for potentials up to 2.2 V *vs* Ag/AgCl by using nanocrystalline $Co_3O_4$ (Lu and Zhao, 2013). Some studies also showed that the synthesis of a compos ite CNT material (PVDF/CNT on PTFE filter (Gao et al., 2014) or PANI as conductive polymer mixed with CNTs (Duan et al., 2016)) increased the lifetime of CNTs used as REMs.

In addition, REMs based on $Ti_4O_7$ seem to be the most promising materials in water treatment applications. In fact, $Ti_4O_7$ has sig nificant resistance to corrosion in alkaline or acidic media, and can be used as either an anode or cathode (Pollock et al., 1984). How ever, $Ti_4O_7$ is not totally immune to passivation phenomenon. Based on stoichiometry, the proportion of $Ti^{3+}$ to $Ti^{4+}$ is equivalent in $Ti_4O_7$, but for example, in the study of Pouilleau et al. (1997), XPS analysis indicated a larger proportion of $Ti^{4+}$ at the surface (the surveyed thickness is a few nm with this technique). Thus, these results suggested that a natural passivation layer of a few nm of $TiO_2$ is spontaneously formed on the $Ti_4O_7$ surface when exposed to ambient air at room temperature (Pouilleau et al., 1997). However, the related mechanisms are neither well understood nor described in the literature. Moreover, data obtained from XPS must be considered with caution, due to the electron beam, which can oxidize the titanium oxide surface. In the literature, the distinction between passivation and corrosion layers (>10 nm) is not well established, and authors commonly use the term of passivation. These passivation or corrosion layers were characterized by *in situ* energy dispersive X ray diffraction (Rowles et al., 2012) or EIS (Waraksa et al., 2003) from 1.6 V *vs.* SHE. Electrochemical analysis appears to be the most relevant method to characterize the dura bility of REMs under anodic polarization. Some studies reported that the passivation was reversible upon cathodic polarization (El Sherif et al., 2010), while other studies reported the contrary (Waraksa et al., 2003). More detailed studies on the passivation and re reduction of Magnéli phases are needed in order to understand how to efficiently manage these anodes during water treatment applications.

## 7. Conclusions

The development of REMs is a breakthrough innovation for electro oxidation processes. The possibility to implement REMs in flow through configurations allows for the advantage of convection enhanced mass transport and high electroactive sur face area. Diffusion limitations usually limiting the efficiency of electro oxidation processes can be minimized. Current efficiencies reported with REMs can reach much higher values than those re ported for conventional 2D electrodes. From the current status of knowledge, it is possible to analyze reaction kinetics in these 3D systems according to a semi empirical approach, which takes into consideration reaction, diffusion and convection rate constants. The development of effective REMs depends on these three parameters. Thus, an ideal REM must present the following characteristics:

Suitable porous structure in order to avoid diffusion limitations (e.g. small pore size) and maintaining a high permeability (e.g. thin active filtration layer, high porosity);
High reactivity, which can be evaluated by determining the electron transfer rate and/or by using probe molecules in order to assess electro oxidation mechanisms (direct electron trans fer, $^{\bullet}OH$ mediated oxidation);
Long lifetime, including fouling and corrosion issues;
Cost effective and environmentally friendly synthesis methods;
Absence of toxicity.

Thus, development of REMs strongly relies on innovations in material science. The use of CNTs has been widely studied mainly because of their high conductivity, and suitable pore structure (high permeability, low pore size). However, corrosion issues occur at high anode potentials and the cytotoxicity of CNTs might prevent their widespread use. Recently, $TiO_x$ materials, known as Magnéli phases, appeared as very promising materials. By comparison to CNTs, corrosion is strongly reduced and their monolithic structure is more compatible to water treatment applications than nano materials. Moreover, the high oxygen overpotential of $TiO_x$ mate rials allows the electro generation of large quantities of $^{\bullet}OH$. Improving the reactivity of REMs is currently a critical parameter in order to take full advantage of the increase mass transfer rates. In addition, once the removal of organic compounds is kinetically limited, adverse effects have been reported from (i) the increase of the competition from $O_2$ evolution at high permeate flux and (ii) electropolymerization phenomena and presence of organic com pounds refractory to direct electron transfer in the REM layer where $^{\bullet}OH$ cannot be generated because of potential drop in the REM depth.

Recent advances in REMs open the way towards broader ap plications of electro oxidation processes for the removal of organic pollutants. Therefore, scientists and engineers must face several challenges in the near future. Particularly, here are some critical points that must be addressed:

Development of REM materials with suitable characteristics, as described above;
Improving the understanding of reactive transport in REMs including a rigorous analysis of reaction kinetics and mass transport in flow through REMs, which is complicated by the variation of the electrode potential according to the electrode depth;
Investigation of the efficiency of the process for the treatment of different real effluents;
Evaluation of the formation of toxic by products, such as per chlorates or halogenated organic compounds, because one of the main drawbacks of electro oxidation processes is the po tential formation of toxic byproducts;
Investigation of the long term lifetime of REMs and imple mentation of procedures for preventing fouling and corrosion issues, if necessary;
Complete life cycle analysis of the process in order to assess the competitiveness of the process, by comparison to other technologies.

These studies are required for the identification of an optimal process configuration. Then, it will be possible to determine the potential of REMs for application in full scale water treatment.

## Acknowledgment

We gratefully acknowledge the National French Agency of Research 'ANR' for funding the project ECO TS/CElectrON (ANR 13

ECOT 003). Clément Trellu particularly thanks the agency for post doctoral fellowship. Funding for Brian P. Chaplin was provided by the National Science Foundation (Grants CBET 1604776 and CBET 1453081 (CAREER)).

## References


Ahmed, F., Lalia, B.S., Kochkodan, V., Hilal, N., Hashaikeh, R., 2016. Electrically conductive polymeric membranes for fouling prevention and detection: a review. Desalination 391, 1 15.

Alkire, R., Gracon, B., 1975. Flow-through porous electrodes. J. Electrochem. Soc. 122, 1594 1601.

Ammar, S., Oturan, M.A., Labiadh, L., Guersalli, A., Abdelhedi, R., Oturan, N., Brillas, E., 2015. Degradation of tyrosol by a novel electro-Fenton process using pyrite as heterogeneous source of iron catalyst. Water Res. 74, 77 87.

Andersson, S., Collen, B., Kuylenstierna, U., Magneli, A., 1957. Phase analysis studies on the titanium-oxygen system. Acta Chem. Scand. Den. Divid. Acta Chem Scand Ser Ser B 11.

Antropov, L., 1972. Theoretical Electrochemistry. Beekman Books, Incorporated.

Ayadi, S., Jedidi, I., Rivallin, M., Gillot, F., Lacour, S., Cerneaux, S., Cretin, M., Ben Amar, R., 2013. Elaboration and characterization of new conductive porous graphite membranes for electrochemical advanced oxidation processes. J. Membr. Sci. 446, 42 49.

Bakr, A.R., Rahaman, M.S., 2016. Electrochemical efficacy of a carboxylated multi-walled carbon nanotube filter for the removal of ibuprofen from aqueous solutions under acidic conditions. Chemosphere 153, 508 520.

Bakr, A.R., Rahaman, M.S., 2017. Removal of bisphenol A by electrochemical carbon-nanotube filter: influential factors and degradation pathway. Chemosphere 185, 879 887.

Banuelos, J.A., Rodríguez, F.J., Manríquez Rocha, J., Bustos, E., Rodríguez, A., Cruz, J.C., Arriaga, L.G., Godínez, L.A., 2013. Novel electro-Fenton approach for regeneration of activated carbon. Environ. Sci. Technol. 47, 7927 7933.

Bard, A.J., Faulkner, L.R., 2000. Electrochemical Methods: Fundamentals and Applications. Wiley.

Bejan, D., Malcolm, J.D., Morrison, L., Bunce, N.J., 2009. Mechanistic investigation of the conductive ceramic Ebonex® as an anode material. Electrochim. Acta 54, 5548 5556.

Belhadj Tahar, N., Savall, A., 2009a. Electrochemical removal of phenol in alkaline solution. Contribution of the anodic polymerization on different electrode materials. Electrochim. Acta 54, 4809 4816.

Belhadj Tahar, N., Savall, A., 2009b. Electropolymerization of phenol on a vitreous carbon electrode in alkaline aqueous solution at different temperatures. Electrochim. Acta 55, 465 469.

Brillas, E., Martínez-Huitle, C.A., 2015. Decontamination of wastewaters containing synthetic organic dyes by electrochemical methods. An updated review. Appl. Catal. B Environ. 166 167, 603 643.

Brillas, E., Sirés, I., Arias, C., Cabot, P.L., Centellas, F., Rodríguez, R.M., Garrido, J.A., 2005. Mineralization of paracetamol in aqueous medium by anodic oxidation with a boron-doped diamond electrode. Chemosphere 58, 399 406.

Brillas, E., Angel Banos, M., Skoumal, M., Lluis Cabot, P., Antonio Garrido, J., Maria Rodriguez, R., 2007. Degradation of the herbicide 2,4-DP by anodic oxidation, electro-Fenton and photoelectro-Fenton using platinum and boron-doped diamond anodes. Chemosphere 68, 199 209.

Brillas, E., Sirés, I., Oturan, M.A., 2009. Electro-Fenton process and related electrochemical technologies based on Fenton's reaction chemistry. Chem. Rev. 109, 6570 6631.

Buxton, G., Greenstock, C., Helman, W., Ross, A., 1988. Critical-review of rate constants for reactions of hydrated electrons, hydrogen-atoms and hydroxyl radicals (.oh/.o-) in aqueous-solution. J. Phys. Chem. Ref. Data 17, 513 886.

Canizares, P., Garcia-Gomez, J., Lobato, J., Rodrigo, M.A., 2003. Electrochemical oxidation of aqueous carboxylic acid wastes using diamond thin-film electrodes. Ind. Eng. Chem. Res. 42, 956 962.

Canizares, P., García-Gómez, J., Fernández de Marcos, I., Rodrigo, M.A., Lobato, J., 2006. Measurement of mass-transfer coefficients by an electrochemical technique. J. Chem. Educ. 83, 1204.

Castro Neto, A.H., Guinea, F., Peres, N.M.R., Novoselov, K.S., Geim, A.K., 2009. The electronic properties of graphene. Rev. Mod. Phys. 81, 109 162.

Chaplin, B.P., 2014. Critical Review of Electrochemical Advanced Oxidation Processes for Water Treatment Applications. Environ. Sci. Process. Impacts.

Comninellis, C., Nerini, A., 1995. Anodic oxidation of phenol in the presence of NaCl for waste-water treatment. J. Appl. Electrochem. 25, 23 28.

Comninellis, C., Pulgarin, C., 1991. Anodic oxidation of phenol for waste water treatment. J. Appl. Electrochem. 21, 703 708.

Comninellis, C., Kapalka, A., Malato, S., Parsons, S.A., Poulios, I., Mantzavinos, D., 2008. Advanced oxidation processes for water treatment: advances and trends for R&D. J. Chem. Technol. Biotechnol. 83, 769 776.

Costa, A.R., de Pinho, M.N., Elimelech, M., 2006. Mechanisms of colloidal natural organic matter fouling in ultrafiltration. J. Membr. Sci. 281, 716 725.

Dashtban Kenari, S.L., Barbeau, B., 2016. Understanding ultrafiltration fouling of ceramic and polymeric membranes caused by oxidized iron and manganese in water treatment. J. Membr. Sci. 516, 1 12.

De Angelis, L., de Cortalezzi, M.M.F., 2013. Ceramic membrane filtration of organic compounds: effect of concentration, pH, and mixtures interactions on fouling. Separ. Purif. Technol. 118, 762 775.

de Oliveira, G.R., Fernandes, N.S., Melo, J.V., de, da Silva, D.R., Urgeghe, C., Martínez-Huitle, C.A., 2011. Electrocatalytic properties of Ti-supported Pt for decolorizing and removing dye from synthetic textile wastewaters. Chem. Eng. J. 168, 208 214.

Dilaver, M., Hocaoğlu, S.M., Soydemir, G., Dursun, M., Keskinler, B., Koyuncu, I., Ağtaş, M., 2018. Hot wastewater recovery by using ceramic membrane ultrafiltration and its reusability in textile industry. J. Clean. Prod. 171, 220 233.

Donaghue, A., Chaplin, B.P., 2013. Effect of select organic compounds on perchlorate formation at boron-doped diamond film anodes. Environ. Sci. Technol. 47, 12391 12399.

dos Santos, E.V., Sena, S.F.M., da Silva, D.R., Ferro, S., De Battisti, A., Martínez-Huitle, C.A., 2014. Scale-up of electrochemical oxidation system for treatment of produced water generated by Brazilian petrochemical industry. Environ. Sci. Pollut. Res. Int. 21, 8466 8475.

Duan, W., Ronen, A., Walker, S., Jassby, D., 2016. Polyaniline-coated carbon nanotube ultrafiltration membranes: enhanced anodic stability for in situ cleaning and electro-oxidation processes. ACS Appl. Mater. Interfaces 8, 22574 22584.

El-Sherif, S., Bejan, D., Bunce, N.J., 2010. Electrochemical oxidation of sulfide ion in synthetic sour brines using periodic polarity reversal at Ebonex® electrodes. Can. J. Chem. 88, 928 936.

Fan, L., Harris, J.L., Roddick, F.A., Booker, N.A., 2001. Influence of the characteristics of natural organic matter on the fouling of microfiltration membranes. Water Res. 35, 4455 4463.

Fan, L., Zhou, Y., Yang, W., Chen, G., Yang, F., 2008. Electrochemical degradation of aqueous solution of Amaranth azo dye on ACF under potentiostatic model. Dyes Pigments 76, 440 446.

Fedkiw, P.S., 1981. Ohmic potential drop in flow-through and flow-by porous electrodes. J. Electrochem. Soc. 128, 831 838.

Fernandes, A., Pacheco, M.J., Ciríaco, L., Lopes, A., 2012. Anodic oxidation of a biologically treated leachate on a boron-doped diamond anode. J. Hazard Mater. 199 200, 82 87.

Ferreira, M., Varela, H., Torresi, R.M., Tremiliosi-Filho, G., 2006. Electrode passivation caused by polymerization of different phenolic compounds. Electrochim. Acta 52, 434 442.

Formoso, P., Pantuso, E., De Filpo, G., Nicoletta, F.P., 2017. Electro-conductive membranes for permeation enhancement and fouling mitigation: a short review. Membranes 7.

Ganiyu, S.O., van Hullebusch, E.D., Cretin, M., Esposito, G., Oturan, M.A., 2015. Coupling of membrane filtration and advanced oxidation processes for removal of pharmaceutical residues: a critical review. Separ. Purif. Technol. 156 (3), 891 914.

Ganiyu, S.O., Le, S., T.X.H., Bechelany, M., Esposito, G., Hullebusch, van, E.D., Oturan, A., Cretin, M., 2017. A hierarchical CoFe-layered double hydroxide modified carbon-felt cathode for heterogeneous electro-Fenton process. J. Mater. Chem. A 5, 3655 3666.

Gao, G., Vecitis, C.D., 2011. Electrochemical carbon nanotube filter oxidative performance as a function of surface chemistry. Environ. Sci. Technol. 45, 9726 9734.

Gao, G., Vecitis, C.D., 2012a. Doped carbon nanotube networks for electrochemical filtration of aqueous phenol: electrolyte precipitation and phenol polymerization. ACS Appl. Mater. Interfaces 4, 1478 1489.

Gao, G., Vecitis, C.D., 2012b. Reactive depth and performance of an electrochemical carbon nanotube network as a function of mass transport. ACS Appl. Mater. Interfaces 4, 6096 6103.

Gao, G., Vecitis, C.D., 2013. Electrocatalysis aqueous phenol with carbon nanotubes networks as anodes: electrodes passivation and regeneration and prevention. Electrochim. Acta 98, 131 138.

Gao, G., Zhang, Q., Vecitis, C.D., 2014. CNT-PVDF composite flow-through electrode for single-pass sequential reduction-oxidation. J. Mater. Chem. A 2, 6185 6190.

Gao, G., Pan, M., Vecitis, C.D., 2015a. Effect of the oxidation approach on carbon nanotube surface functional groups and electrooxidative filtration performance. J. Mater. Chem. A 3, 7575 7582.

Gao, G., Zhang, Q., Hao, Z., Vecitis, C.D., 2015b. Carbon nanotube membrane stack for flow-through sequential regenerative electro-Fenton. Environ. Sci. Technol. 49, 2375 2383.

Geng, P., Chen, G., 2016. Magnéli Ti4O7 modified ceramic membrane for electrically-assisted filtration with antifouling property. J. Membr. Sci. 498, 302 314.

Geng, P., Chen, G., 2017. Antifouling ceramic membrane electrode modified by Magnéli Ti4O7 for electro-microfiltration of humic acid. Separ. Purif. Technol. 185, 61 71.

Graves, J.E., Pletcher, D., Clarke, R.L., Walsh, F.C., 1991. The electrochemistry of Magnéli phase titanium oxide ceramic electrodes Part I. The deposition and properties of metal coatings. J. Appl. Electrochem. 21, 848 857.

Grimm, J., Bessarabov, D., Sanderson, R., 1998. Review of electro-assisted methods for water purification. Desalination 115, 285 294.

Guo, W., Ngo, H.-H., Li, J., 2012. A mini-review on membrane fouling. Bioresour. Technol. 122, 27 34.

Guo, L., Ding, K., Rockne, K., Duran, M., Chaplin, B.P., 2016a. Bacteria inactivation at a sub-stoichiometric titanium dioxide reactive electrochemical membrane. J. Hazard Mater. 319, 137 146.

Guo, L., Jing, Y., Chaplin, B.P., 2016b. Development and characterization of ultrafiltration TiO2 Magnéli phase reactive electrochemical membranes. Environ. Sci. Technol. 50, 1428 1436. https://doi.org/10.1021/acs.est.5b04366.

Hayfield, P.C.S., 2001. Development of a New Material: Monolithic Ti4O7 Ebonex

Ceramic. Royal Society of Chemistry.
Howe, K.J., Clark, M.M., 2002. Fouling of microfiltration and ultrafiltration membranes by natural waters. Environ. Sci. Technol. 36, 3571 3576.
Huotari, H.M., Tragårdh, G., Huisman, I.H., 1999. Crossflow membrane filtration enhanced by an external DC electric field: a review. Chem. Eng. Res. Des. 77, 461 468.
Iijima, S., 1991. Helical microtubules of graphitic carbon. Nature 354, 56.
Iijima, S., Ichihashi, T., 1993. Single-shell carbon nanotubes of 1-nm diameter. Nature 363, 603.
Jing, Y., Chaplin, B.P., 2016. Electrochemical impedance spectroscopy study of membrane fouling characterization at a conductive sub-stoichiometric TiO2 reactive electrochemical membrane: transmission line model development. J. Membr. Sci. 511, 238 249.
Jing, Y., Guo, L., Chaplin, B.P., 2016. Electrochemical impedance spectroscopy study of membrane fouling and electrochemical regeneration at a sub-stoichiometric TiO2 reactive electrochemical membrane. J. Membr. Sci. 510, 510 523.
Joss, A., Siegrist, H., Ternes, T.A., 2008. Are we about to upgrade wastewater treatment for removing organic micropollutants? Water Sci. Technol. 57, 251 255.
Jung, C.-W., Son, H.-J., Kang, L.-S., 2006. Effects of membrane material and pretreatment coagulation on membrane fouling: fouling mechanism and NOM removal. Desalination 197, 154 164.
Kapałka, A., Fóti, G., Comninellis, C., 2008. Kinetic modelling of the electrochemical mineralization of organic pollutants for wastewater treatment. J. Appl. Electrochem. 38, 7 16.
Kapałka, A., Fóti, G., Comninellis, C., 2009. The importance of electrode material in environmental electrochemistry: formation and reactivity of free hydroxyl radicals on boron-doped diamond electrodes. Electrochim. Acta 54, 2018 2023.
Kapałka, A., Fóti, G., Comninellis, C., Chen, G., 2010. Basic principles of the electrochemical mineralization of organic pollutants for wastewater treatment. In: Comninellis, C., Chen, G. (Eds.), Electrochemistry for the Environment. Springer, New York, pp. 1 23.
Kinoshita, K., 1988. Carbon: Electrochemical and Physicochemical Properties. Wiley.
Kitada, A., Hasegawa, G., Kobayashi, Y., Kanamori, K., Nakanishi, K., Kageyama, H., 2012. Selective preparation of macroporous monoliths of conductive titanium oxides TinO2n 1 (n 2, 3, 4, 6). J. Am. Chem. Soc. 134, 10894 10898.
Kolbrecka, K., Przyluski, J., 1994. Sub-stoichiometric titanium oxides as ceramic electrodes for oxygen evolution structural aspects of the voltammetric behaviour of TinO2n−1. Electrochim. Acta 39, 1591 1595.
Korbahti, B.K., Tanyolaç, A., 2003. Continuous electrochemical treatment of phenolic wastewater in a tubular reactor. Water Res. 37, 1505 1514.
Lasia, A., 1997. Porous electrodes in the presence of a concentration gradient. J. Electroanal. Chem. 428, 155 164.
Lasia, A., 2008. Impedance of porous electrodes. ECS Trans. 13, 1 18.
Lee, S.-J., Kim, J.-H., 2014. Differential natural organic matter fouling of ceramic versus polymeric ultrafiltration membranes. Water Res. 48, 43 51.
Lee, N.H., Amy, G., Croue, J.P., Buisson, H., 2004. Identification and understanding of fouling in low-pressure membrane (MF/UF) filtration by natural organic matter (NOM). Water Res. 38, 4511 4523.
Lee, S.-J., Dilaver, M., Park, P.-K., Kim, J.-H., 2013. Comparative analysis of fouling characteristics of ceramic and polymeric microfiltration membranes using filtration models. J. Membr. Sci. 432, 97 105.
Li, D., Tang, J., Zhou, X., Li, J., Sun, X., Shen, J., Wang, L., Han, W., 2016. Electrochemical degradation of pyridine by Ti/SnO2 Sb tubular porous electrode. Chemosphere 149, 49 56.
Li, J., Liu, Q., Liu, Y., Xie, J., 2017. Development of electro-active forward osmosis membranes to remove phenolic compounds and reject salts. Environ. Sci.-Water Res. Technol 3, 139 146.
Liu, H., Vecitis, C.D., 2012. Reactive transport mechanism for organic oxidation during electrochemical filtration: mass-Transfer, physical adsorption, and electron-transfer. J. Phys. Chem. C 116, 374 383.
Liu, H., Vajpayee, A., Vecitis, C.D., 2013. Bismuth-doped tin oxide-coated carbon nanotube network: improved anode stability and efficiency for flow-through organic electrooxidation. ACS Appl. Mater. Interfaces 5, 10054 10066.
Liu, Y., Lee, J.H.D., Xia, Q., Ma, Y., Yu, Y., Yung, L.Y.L., Xie, J., Nam Ong, C., Vecitis, D., Zhou, Z., 2014. A graphene-based electrochemical filter for water purification. J. Mater. Chem. A 2, 16554 16562.
Liu, Y., Liu, H., Zhou, Z., Wang, T., Ong, C.N., Vecitis, C.D., 2015. Degradation of the common aqueous antibiotic tetracycline using a carbon nanotube electrochemical filter. Environ. Sci. Technol. 49, 7974 7980.
Liu, Z., Zhu, M., Wang, Z., Wang, H., Deng, C., Li, K., 2016a. Effective degradation of aqueous tetracycline using a nano-TiO2/carbon electrocatalytic membrane. Materials 9, 364.
Liu, Z., Zhu, M., Wang, Z., Wang, H., Deng, C., Li, K., 2016b. Novel antimony doped tin oxide/carbon aerogel as efficient electrocatalytic filtration membrane. AIP Adv. 6, 055015.
Liu, Z., Zhu, M., Zhao, L., Deng, C., Ma, J., Wang, Z., Liu, H., Wang, H., 2017. Aqueous tetracycline degradation by coal-based carbon electrocatalytic filtration membrane: effect of nano antimony-doped tin dioxide coating. Chem. Eng. J. 314, 59 68.
Lu, X., Zhao, C., 2013. Highly efficient and robust oxygen evolution catalysts achieved by anchoring nanocrystalline cobalt oxides onto mildly oxidized multi-walled carbon nanotubes. J. Mater. Chem. A 1, 12053 12059.
Lu, Y., Matsuda, Y., Sagara, K., Hao, L., Otomitsu, T., Yoshida, H., 2012. Fabrication and thermoelectric properties of magneli phases by adding Ti into TiO2. Adv. Mater. Res. 415 417, 1291 1296.
Luo, Y., Guo, W., Ngo, H.H., Nghiem, L.D., Hai, F.I., Zhang, J., Liang, S., Wang, X.C., 2014. A review on the occurrence of micropollutants in the aquatic environment and their fate and removal during wastewater treatment. Sci. Total Environ. 473, 619 641.
Mameda, N., Park, H.-J., Choo, K.-H., 2017. Membrane electro-oxidizer: a new hybrid membrane system with electrochemical oxidation for enhanced organics and fouling control. Water Res. 126, 40 49.
Martínez-Huitle, C.A., Ferro, S., 2006. Electrochemical oxidation of organic pollutants for the wastewater treatment: direct and indirect processes. Chem. Soc. Rev. 35, 1324 1340.
Martínez-Huitle, C.A., Rodrigo, M.A., Sirés, I., Scialdone, O., 2015. Single and coupled electrochemical processes and reactors for the abatement of organic water pollutants: a critical review. Chem. Rev. 115, 13362 13407.
Mascia, M., Vacca, A., Palmas, S., Polcaro, A.M., 2007. Kinetics of the electrochemical oxidation of organic compounds at BDD anodes: modelling of surface reactions. J. Appl. Electrochem. 37, 71 76.
Miller-Folk, R.R., Noftle, R.E., Pletcher, D., 1989. Electron transfer reactions at Ebonex ceramic electrodes. J. Electroanal. Chem. Interfacial Electrochem. 274, 257 261.
Nayak, S., Chaplin, B.P., 2018. Fabrication and characterization of porous, conductive, monolithic Ti4O7 electrodes. Electrochim. Acta 263, 299 310.
Novoselov, K.S., Geim, A.K., Morozov, S.V., Jiang, D., Zhang, Y., Dubonos, S.V., Grigorieva, I.V., Firsov, A.A., 2004. Electric field effect in atomically thin carbon films. Science 306, 666 669.
Ohmori, S., Saito, T., 2012. Electrochemical durability of single-wall carbon nanotube electrode against anodic oxidation in water. Carbon 50, 4932 4938.
Oturan, N., Brillas, E., Oturan, M.A., 2012. Unprecedented total mineralization of atrazine and cyanuric acid by anodic oxidation and electro-Fenton with a boron-doped diamond anode. Environ. Chem. Lett. 10, 165 170.
Ozcan, A., Sahin, Y., Koparal, A.S., Oturan, M.A., 2008. Propham mineralization in aqueous medium by anodic oxidation using boron-doped diamond anode: influence of experimental parameters on degradation kinetics and mineralization efficiency. Water Res. 42, 2889 2898.
Padilha, A.C.M., Raebiger, H., Rocha, A.R., Dalpian, G.M., 2016. Charge storage in oxygen deficient phases of $TiO_2$: defect physics without defects. Sci. Rep. 6, 28871.
Panizza, M., Cerisola, G., 2009. Direct and mediated anodic oxidation of organic pollutants. Chem. Rev. 109, 6541 6569.
Panizza, M., Michaud, P.A., Cerisola, G., Comninellis, C., 2001. Anodic oxidation of 2-naphthol at boron-doped diamond electrodes. J. Electroanal. Chem. 507, 206 214.
Panizza, M., Barbucci, A., Ricotti, R., Cerisola, G., 2007. Electrochemical degradation of methylene blue. Separ. Purif. Technol. 54, 382 387.
Panizza, M., Kapalka, A., Comninellis, C., 2008. Oxidation of organic pollutants on BDD anodes using modulated current electrolysis. Electrochim. Acta 53, 2289 2295.
Peigney, A., Laurent, C., Flahaut, E., Bacsa, R.R., Rousset, A., 2001. Specific surface area of carbon nanotubes and bundles of carbon nanotubes. Carbon 39, 507 514.
Pollock, R.J., Houlihan, J.F., Bain, A.N., Coryea, B.S., 1984. Electrochemical properties of a new electrode material, Ti4O7. Mater. Res. Bull. 19, 17 24.
Pouilleau, J., Devilliers, D., Groult, H., Marcus, P., 1997. Surface study of a titanium-based ceramic electrode material by X-ray photoelectron spectroscopy. J. Mater. Sci. 32, 5645 5651.
Prasek, J., Drbohlavova, J., Chomoucka, J., Hubalek, J., Jasek, O., Adam, V., Kizek, R., 2011. Methods for carbon nanotubes synthesis review. J. Mater. Chem. 21, 15872 15884.
Radjenovic, J., Sedlak, D.L., 2015. Challenges and opportunities for electrochemical processes as next-generation technologies for the treatment of contaminated water. Environ. Sci. Technol. 49, 11292 11302.
Ren, G., Zhou, M., Liu, M., Ma, L., Yang, H., 2016. A novel vertical-flow electro-Fenton reactor for organic wastewater treatment. Chem. Eng. J. 298, 55 67.
Risch, T., Newman, J., 1984. A theoretical comparison of flow-through and flow-by porous electrodes at the limiting current. J. Electrochem. Soc. 131, 2551 2556.
Rodrigo, M.A., Michaud, P.A., Duo, I., Panizza, M., Cerisola, G., Comninellis, C., 2001. Oxidation of 4-chlorophenol at boron-doped diamond electrode for wastewater treatment. J. Electrochem. Soc. 148, D60 D64.
Ronen, A., Walker, S.L., Jassby, D., 2016. Electroconductive and electroresponsive membranes for water treatment. Rev. Chem. Eng. 32.
Rowles, M.R., Styles, M.J., Madsen, I.C., Scarlett, N.V.Y., McGregor, K., Riley, D.P., Snook, G.A., Urban, A.J., Connolley, T., Reinhard, C., 2012. Quantification of passivation layer growth in inert anodes for molten salt electrochemistry by in situ energy-dispersive diffraction. J. Appl. Crystallogr. 45, 28 37.
Saleh, M.M., 2007. Simulation of oxygen evolution reaction at porous anode from flowing electrolytes. J. Solid State Electrochem. 11, 811 820.
Santos, M.C., Elabd, Y.A., Jing, Y., Chaplin, B.P., Fang, L., 2016. Highly porous Ti4O7 reactive electrochemical water filtration membranes fabricated via electrospinning/electrospraying. AIChE J. 62, 508 524.
Schnoor, M.H., Vecitis, C.D., 2013. Quantitative examination of aqueous ferrocyanide oxidation in a carbon nanotube electrochemical filter: effects of flow rate, ionic strength, and cathode material. J. Phys. Chem. C 117, 2855 2867.
Shvedova, A., Castranova, V., Kisin, E., Schwegler-Berry, D., Murray, A., Gandelsman, V., Maynard, A., Baron, P., 2003. Exposure to carbon nanotube material: assessment of nanotube cytotoxicity using human keratinocyte cells. J. Toxicol. Environ. Health A 66, 1909 1926.
Siahrostami, S., Li, G.-L., Viswanathan, V., Nørskov, J.K., 2017. One- or two-electron

water oxidation, hydroxyl radical, or H2O2 evolution. J. Phys. Chem. Lett. 8, 1157 1160.
Sirés, I., Brillas, E., Oturan, M.A., Rodrigo, M.A., Panizza, M., 2014. Electrochemical advanced oxidation processes: today and tomorrow. A review. Environ. Sci. Pollut. Res. 21, 8336 8367.
Smith, J.R., Walsh, F.C., Clarke, R.L., 1998. Electrodes based on Magnéli phase titanium oxides: the properties and applications of Ebonex® materials. J. Appl. Electrochem. 28, 1021 1033.
Sun, X., Wu, J., Chen, Z., Su, X., Hinds, B.J., 2013. Fouling characteristics and electrochemical recovery of carbon nanotube membranes. Adv. Funct. Mater. 23, 1500 1506.
Tang, C., Zhou, D., Zhang, Q., 2012. Synthesis and characterization of Magneli phases: reduction of TiO2 in a decomposed NH3 atmosphere. Mater. Lett. 79, 42 44.
Tominaga, M., Yatsugi, Y., Watanabe, N., 2014. Oxidative corrosion potential vs. pH diagram for single-walled carbon nanotubes. RSC Adv. 4, 27224 27227.
Trainham, J.A., Newman, J., 1977a. A flow-through porous electrode model: application to metal-ion removal from dilute streams. J. Electrochem. Soc. 124, 1528 1540.
Trainham, J.A., Newman, J., 1977b. A thermodynamic estimation of the minimum concentration attainable in a flow-through porous electrode reactor. J. Appl. Electrochem. 7, 287 297.
Trainham, J.A., Newman, J., 1978. The effect of electrode placement and finite matrix conductivity on the performance of flow-through porous electrodes. J. Electrochem. Soc. 125, 58 68.
Trellu, C., Ganzenko, O., Papirio, S., Pechaud, Y., Oturan, N., Huguenot, D., van Hullebusch, E.D., Esposito, G., Oturan, M.A., 2016a. Combination of anodic oxidation and biological treatment for the removal of phenanthrene and Tween 80 from soil washing solution. Chem. Eng. J. 306, 588 596.
Trellu, C., Péchaud, Y., Oturan, N., Mousset, E., Huguenot, D., Hullebusch, E.D., van, Esposito, G., Oturan, M.A., 2016b. Comparative study on the removal of humic acids from drinking water by anodic oxidation and electro-Fenton processes: mineralization efficiency and modelling. Appl. Catal. B Environ. 194, 32 41.
Trellu, C., Coetsier, C., Rouch, J.-C., Esmilaire, R., Rivallin, M., Cretin, M., Causserand, C., 2018. Mineralization of organic pollutants by anodic oxidation using reactive electrochemical membrane synthesized from carbothermal reduction of TiO2. Water Res. 131, 310 319.
Vasudevan, S., Oturan, M.A., 2014. Electrochemistry: as cause and cure in water pollution an overview. Environ. Chem. Lett. 12, 97 108.
Vecitis, C.D., Gao, G., Liu, H., 2011. Electrochemical carbon nanotube filter for adsorption, desorption, and oxidation of aqueous dyes and anions. J. Phys. Chem. C 115, 3621 3629.
Wang, F., Tarabara, V.V., 2008. Pore blocking mechanisms during early stages of membrane fouling by colloids. J. Colloid Interface Sci. 328, 464 469.
Wang, B., Tang, J., Wang, F., 1987. Electrochemical polymerization of aniline. Synth. Met. 18, 323 328.
Wang, H., Guan, Q., Li, J., Wang, T., 2014. Phenolic wastewater treatment by an electrocatalytic membrane reactor. Catal. Today 236, 121 126.
Waraksa, C.C., Chen, G., Macdonald, D.D., Mallouk, T.E., 2003. EIS studies of porous oxygen electrodes with discrete particles II. Transmission line modeling. J. Electrochem. Soc. 150, E429 E437.
Wilson, E.J., Geankoplis, C.J., 1966. Liquid mass transfer at very low Reynolds numbers in packed beds. Ind. Eng. Chem. Fundam. 5, 9 14.
Wu, Z., Chen, H., Dong, Y., Mao, H., Sun, J., Chen, S., Craig, V.S.J., Hu, J., 2008. Cleaning using nanobubbles: defouling by electrochemical generation of bubbles. J. Colloid Interface Sci. 328, 10 14.
Xiao, K., Wang, X., Huang, X., Waite, T.D., Wen, X., 2011. Combined effect of membrane and foulant hydrophobicity and surface charge on adsorptive fouling during microfiltration. J. Membr. Sci. 373, 140 151.
Xu, A., Han, W., Li, J., Sun, X., Shen, J., Wang, L., 2016. Electrogeneration of hydrogen peroxide using Ti/IrO2 Ta2O5 anode in dual tubular membranes Electro-Fenton reactor for the degradation of tricyclazole without aeration. Chem. Eng. J. 295, 152 159.
Yamamura, H., Kimura, K., Watanabe, Y., 2007. Mechanism involved in the evolution of physically irreversible fouling in microfiltration and ultrafiltration membranes used for drinking water treatment. Environ. Sci. Technol. 41, 6789 6794.
Yanez, J.E.H., Wang, Z., Lege, S., Obst, M., Roehler, S., Burkhardt, C.J., Zwiener, C., 2017. Application and characterization of electroactive membranes based on carbon nanotubes and zerovalent iron nanoparticles. Water Res. 108, 78 85.
Yang, J., Wang, J., Jia, J., 2009. Improvement of electrochemical wastewater treatment through mass transfer in a seepage carbon nanotube electrode reactor. Environ. Sci. Technol. 43, 3796 3802.
Yang, Y., Li, J., Wang, H., Song, X., Wang, T., He, B., Liang, X., Ngo, H.H., 2011. An electrocatalytic membrane reactor with self-cleaning function for industrial wastewater treatment. Angew. Chem. Int. Ed. 50, 2148 2150.
Yang, Y., Wang, H., Li, J., He, B., Wang, T., Liao, S., 2012. Novel functionalized nano-TiO2 loading electrocatalytic membrane for oily wastewater treatment. Environ. Sci. Technol. 46, 6815 6821.
Yang, X., Kirsch, J., Fergus, J., Simonian, A., 2013. Modeling analysis of electrode fouling during electrolysis of phenolic compounds. Electrochim. Acta 94, 259 268.
Ye, J., Wang, G., Li, X., Liu, Y., Zhu, R., 2015. Temperature effect on electrochemical properties of Ti4O7 electrodes prepared by spark plasma sintering. J. Mater. Sci. Mater. Electron. 26, 4683 4690.
Yi, Y., Tornow, J., Willinger, E., Willinger, M.G., Ranjan, C., Schlogl, R., 2015. Electrochemical degradation of multiwall carbon nanotubes at high anodic potential for oxygen evolution in acidic media. ChemElectroChem 2, 1929 1937.
You, S., Liu, B., Gao, Y., Wang, Y., Tang, C.Y., Huang, Y., Ren, N., 2016. Monolithic porous Magnéli-phase Ti4O7 for electro-oxidation treatment of industrial wastewater. Electrochim. Acta 214, 326 335.
Yuan, W., Kocic, A., Zydney, A.L., 2002. Analysis of humic acid fouling during microfiltration using a pore blockage cake filtration model. J. Membr. Sci. 198, 51 62.
Zaky, A.M., Chaplin, B.P., 2013. Porous substoichiometric TiO2 anodes as reactive electrochemical membranes for water treatment. Environ. Sci. Technol. 47, 6554 6563.
Zaky, A.M., Chaplin, B.P., 2014. Mechanism of p-substituted phenol oxidation at a Ti4O7 reactive electrochemical membrane. Environ. Sci. Technol. 48, 5857 5867.
Zhang, Q., Vecitis, C.D., 2014. Conductive CNT-PVDF membrane for capacitive organic fouling reduction. J. Membr. Sci. 459, 143 156.
Zhang, Y., Wei, K., Han, W., Sun, X., Li, J., Shen, J., Wang, L., 2016. Improved electrochemical oxidation of tricyclazole from aqueous solution by enhancing mass transfer in a tubular porous electrode electrocatalytic reactor. Electrochim. Acta 189, 1 8.
Zhao, G., Zhang, Y., lei, Y., Lv, B., Gao, J., Zhang, Y., Li, D., 2010. Fabrication and electrochemical treatment application of a novel lead dioxide anode with superhydrophobic surfaces, high oxygen evolution potential, and oxidation capability. Environ. Sci. Technol. 44, 1754 1759.
Zhao, F., Liu, L., Yang, F., Ren, N., 2013. E-Fenton degradation of MB during filtration with Gr/PPy modified membrane cathode. Chem. Eng. J. 230, 491 498.
Zhou, X., Liu, S., Xu, A., Wei, K., Han, W., Li, J., Sun, X., Shen, J., Liu, X., Wang, L., 2017. A multi-walled carbon nanotube electrode based on porous Graphite-RuO2 in electrochemical filter for pyrrole degradation. Chem. Eng. J. 330, 956 964.
Zhu, R., Liu, Y., Ye, J., Zhang, X., 2013. Magnéli phase Ti4O7 powder from carbothermal reduction method: formation, conductivity and optical properties. J. Mater. Sci. Mater. Electron. 12, 4853 4856.